



**HAL**  
open science

## Targeting lung macrophages for fungal and parasitic pulmonary infections with innovative amphotericin B dry powder inhalers

E. de Pablo, P. O'Connell, R. Fernández-García, S. Marchand, A. Chauzy, F. Tewes, M.A. Dea-Ayuela, D. Kumar, F. Bolás, M.P. Ballesteros, et al.

► **To cite this version:**

E. de Pablo, P. O'Connell, R. Fernández-García, S. Marchand, A. Chauzy, et al.. Targeting lung macrophages for fungal and parasitic pulmonary infections with innovative amphotericin B dry powder inhalers. *International Journal of Pharmaceutics*, 2023, 635, pp.122788. 10.1016/j.ijpharm.2023.122788 . hal-04131635

**HAL Id: hal-04131635**

**<https://hal.science/hal-04131635v1>**

Submitted on 10 Jul 2024

**HAL** is a multi-disciplinary open access archive for the deposit and dissemination of scientific research documents, whether they are published or not. The documents may come from teaching and research institutions in France or abroad, or from public or private research centers.

L'archive ouverte pluridisciplinaire **HAL**, est destinée au dépôt et à la diffusion de documents scientifiques de niveau recherche, publiés ou non, émanant des établissements d'enseignement et de recherche français ou étrangers, des laboratoires publics ou privés.



Distributed under a Creative Commons Attribution - NonCommercial - NoDerivatives 4.0 International License



## Targeting lung macrophages for fungal and parasitic pulmonary infections with innovative amphotericin B dry powder inhalers

E. de Pablo<sup>a</sup>, P. O'Connell<sup>b</sup>, R. Fernández-García<sup>a</sup>, S. Marchand<sup>c,d</sup>, A. Chauzy<sup>c</sup>, F. Tewes<sup>c,d</sup>, M.A. Dea-Ayuela<sup>e</sup>, D. Kumar<sup>f</sup>, F. Bolás<sup>g</sup>, M.P. Ballesteros<sup>a,h</sup>, J.J. Torrado<sup>a,h</sup>, A.M. Healy<sup>b</sup>, D. R. Serrano<sup>a,h,\*</sup>

<sup>a</sup> Pharmaceutics and Food Technology Department, School of Pharmacy, Universidad Complutense de Madrid, Plaza Ramón y Cajal s/n, 28040 Madrid, Spain

<sup>b</sup> School of Pharmacy and Pharmaceutical Sciences, Trinity College Dublin, Dublin 2, Ireland

<sup>c</sup> UMR 1070, Université de PoitiersPôle Biologie Santé, 1, Rue Georges Bonnet, 86073 Poitiers, France

<sup>d</sup> Laboratoire de Toxicologie-Pharmacocinétique, CHU de Poitiers, 2, Rue de la milétrie, 86021 Poitiers, France

<sup>e</sup> Pharmacy Department, School of Life Sciences, Universidad Cardenal Herrera-CEU, Moncada 46113 Valencia, Spain

<sup>f</sup> Department of Pharmaceutical Engineering & Technology, Indian Institute of Technology (Banaras Hindu University), Varanasi, India

<sup>g</sup> Parasitology Department, School of Pharmacy, Universidad Complutense de Madrid, Plaza Ramón y Cajal s/n, 28040 Madrid, Spain

<sup>h</sup> Instituto Universitario de Farmacia Industrial, Facultad de Farmacia, Universidad Complutense de Madrid, 28040 Madrid, Spain

### ARTICLE INFO

#### Keywords:

Amphotericin B  
Pulmonary administration  
Spray drying  
Dry powder inhaler  
ASAP  
Amorphous  
Crystalline

### ABSTRACT

The incidence of fungal pulmonary infections is known to be on the increase, and yet there is an alarming gap in terms of marketed antifungal therapies that are available for pulmonary administration. Amphotericin B (AmB) is a highly efficient broad-spectrum antifungal only marketed as an intravenous formulation. Based on the lack of effective antifungal and antiparasitic pulmonary treatments, the aim of this study was to develop a carbohydrate-based AmB dry powder inhaler (DPI) formulation, prepared by spray drying. Amorphous AmB microparticles were developed by combining 39.7 % AmB with 39.7 %  $\gamma$ -cyclodextrin, 8.1 % mannose and 12.5 % leucine. An increase in the mannose concentration from 8.1 to 29.8 %, led to partial drug crystallisation. Both formulations showed good *in vitro* lung deposition characteristics (80 % FPF < 5  $\mu$ m and MMAD < 3  $\mu$ m) at different air flow rates (60 and 30 L/min) when used with a DPI, but also during nebulisation upon reconstitution in water.

### 1. Introduction

Every day, we inhale many types of particles that are circulating in the environment, including spores, which are single dormant fungal cells. In immunocompromised, transplant, cancer or HIV patients, these spores can colonize high, medium and low regions of the respiratory tract (RT) causing fungal lung infections (de Pablo et al., 2017; Orphan designation: Amphotericin B (for inhalation use)EMA 28/08/2006). Symptoms of pulmonary fungal infection (such as aspergillosis) are shortness of breath, chest pain, cough, fever, and weight loss. Pulmonary fungal infections are life-threatening due to the high risk of severe pulmonary disease and fungal sepsis (Orphan designation: Amphotericin B (for inhalation use)EMA 28/08/2006).

Patients with disseminated leishmaniasis, a disease caused by an intracellular protozoan parasite from genus *Leishmania*, can also suffer

from severe pulmonary symptoms such as bilateral pleural effusions specially in those cases where parasites are spread even to the lung contained in alveolar macrophages (Chenoweth et al., 1993).

Amphotericin B (AmB) is the gold-standard drug currently utilized in the treatment of fungal pulmonary infections and leishmaniasis due to its broad-spectrum activity and low resistance. Its mechanism of action is based on the selective binding to ergosterol present in the cell plasma membranes of fungi and some parasites, such as *Leishmania*. AmB self-assembles on the membrane, forming pores that lead to loss of small cations, particularly  $K^+$ , causing cell death (Ordóñez-Gutiérrez et al., 2007). In spite of its selectivity for ergosterol, AmB can also bind to cholesterol present in mammalian cells causing toxicity, in particular nephrotoxicity, as kidney cell membranes are rich in cholesterol (Ruiz et al., 2014).

Formulating AmB is challenging, due to its large molecular weight

\* Corresponding author at: Pharmaceutics and Food Technology Department, School of Pharmacy, Universidad Complutense de Madrid, Plaza Ramón y Cajal s/n, 28040 Madrid, Spain.

E-mail address: [drserran@ucm.es](mailto:drserran@ucm.es) (D.R. Serrano).

<https://doi.org/10.1016/j.ijpharm.2023.122788>

Received 4 November 2022; Received in revised form 24 February 2023; Accepted 25 February 2023

Available online 1 March 2023

0378-5173/© 2023 The Authors. Published by Elsevier B.V. This is an open access article under the CC BY-NC-ND license (<http://creativecommons.org/licenses/by-nc-nd/4.0/>).

(924 kDa), low aqueous solubility at physiological pH (<1mg/L), low membrane permeability ( $\log = 0.95$ ) and its zwitterionic and amphiphilic nature associated with an asymmetrical distribution of its hydrophilic and hydrophobic groups (Ruiz et al., 2014; Serrano et al., 2015). Currently, AmB is only marketed as a lyophilised powder for extemporaneous reconstitution before intravenous administration. The conventional micellar formulation of AmB (Fungizone®) was replaced in clinical use by lipid-based medicines (AmBisome®, Abelcet® and Amphocil®) due to their improved efficacy/toxicity balance (de Pablo et al., 2017; DrugPatentWatch, 27/09/2010).

However, AmB for inhalation use is not authorised anywhere worldwide. On 28 August 2006, orphan designation (EU/3/06/391) was granted by the European Commission to Nektar Therapeutics UK Ltd, United Kingdom, allowing the use of AmB by oral inhalation for the prevention of pulmonary fungal infections in patients deemed at risk (2.2/10,000 estimated people in the EU) (Orphan designation: Amphotericin B (for inhalation use)EMA, 28/08/2006). To date, marketed lipid-based AmB intravenous medicines are authorised for the treatment and prophylaxis of pulmonary fungal infections; however, these formulations are not designed for pulmonary administration, and require patient hospitalization in order to reconstitute the formulation appropriately by trained personnel and administer it using a suitable nebulizer apparatus (Orphan designation: Amphotericin B (for inhalation use)EMA, 28/08/2006).

Today, there are >400 different inhaled products marketed in Europe and >40 drugs are registered to treat respiratory diseases (EMA). Inhaled medications are administered using pressurised metered-dose inhalers (pMDIs), nebulizers or dry powder inhalers (DPIs) and each device requires a different formulation strategy to ensure successful drug delivery into the lung (Berkenfeld et al., 2015; de Pablo et al., 2017).

Overall, DPIs have several advantages over other inhalation devices such as the consistency of the dose delivered to the airways, good deposition efficiency, ease of administration and formulation stability (Sosnowski, 2016). The main advantage of DPIs over pMDIs is the fact that is not necessary to have hand-breath coordination between the device actuation and patient inhalation (Dickinson et al., 2001). DPIs overcome some disadvantages associated with nebulizers, by lowering the total treatment time, involving easier operational procedures, and lowering overall treatment costs due to better patient compliance, minimal residual drug volumes and better efficiency of drug delivery to the lung (Dickinson et al., 2001). However, one of the limitations of DPI formulations is that the patient inspiratory flow rate determines, to a large extent, the efficiency of inhalation and the drug deposition to the lung [6]. Hence, drugs might not be delivered successfully in patients suffering from severe fungal or parasitic pulmonary infections with a highly decreased pulmonary capacity. In this respect, a versatile DPI formulation that could be both administrated as a DPI or easily reconstituted in water followed by nebulization would be of great advantage, especially for pediatric and geriatric population or other patients with difficulties in achieving a deep inspiration (Vartiainen et al., 2018). The latter strategy based on powder reconstitution in water for nebulization, could be useful in those patients that require dose adjustment, such as for example, in the case of prophylactic treatments or severe infections (Paranjpe & Muller-Goymann, 2014; Rijnders et al., 2008).

The hypothesis underpinning this work is that the development of a DPI formulation containing AmB could deliver the drug directly to the site of action, in particular for the treatment and prophylaxis of fungal lung infections such as those caused by aspergillosis, but also to target the alveolar macrophages and hence, act as an alternative treatment for disseminated leishmaniasis. The development of a carbohydrate AmB-based pulmonary formulation can exert a significant improvement over the currently utilized off-label lipidic AmB-based formulations intended for parenteral use. Patient compliance would be greatly improved as hospitalization would not be necessary. For this reason, the aim of this work was to develop a DPI that is able to deliver AmB along

all regions of the RT (high, medium and low), which is a necessity for the complete eradication of fungal pulmonary infections, but also specifically towards the alveolar macrophages if used in patients with disseminated leishmaniasis.

QbD and DoE was implemented to optimise the flow properties and particle size of the formulations, to ensure optimal lung deposition. Comprehensive physicochemical characterization was carried out including: XRD, FTIR, DSC, MMAD, FPF < 5 and 3  $\mu\text{m}$ , DVS, surface area and stability studies. *In vitro* macrophage uptake and antifungal and antileishmanial activity were tested as well as *in vivo* pharmacokinetic pulmonary bioavailability.

## 2. Materials and methods

### 2.1. Materials

Amphotericin B (AmB) was purchased from Azelis (Barcelona, Spain). Salbutamol sulphate (99.5 % purity) was bought from Fluka BioChemika (Wicklow, Ireland). D-(+)-Mannose and D-(+)-Raffinose with a purity  $\geq 99$  %, were purchased from Sigma Aldrich (Dublin, Ireland). L-Leucine reagent grade with purity  $\geq 98$  %, was purchased from Sigma Aldrich (Dublin, Ireland).  $\gamma$ -Cyclodextrin (CD) Cavamax W8, ISP, with a purity  $\geq 99$  % was a gift from Ashland Industries Europe GmbH (Schaffhausen Switzerland). Sodium deoxycholate was purchased from Fluka Chemie A.G. Buch, Switzerland. Phosphoric acid (85 %) ( $\text{H}_3\text{PO}_4$ ) and sodium hydroxide (NaOH) were purchased from Pan-reac S.A. (Barcelona, Spain). Solvents of HPLC grade were used All other chemicals were of reagent grade and were used without further purification.

### 2.2. Methods

#### 2.2.1. Design of experiments

2.2.1.1. *Defining the target product profile (TPP) and identifying the critical quality attributes (CQAs)*. The TPP is based on the summary of the characteristics of the drug product, as it relates to quality, efficacy and safety. Among the TPP elements that define the key quality characteristics of a pulmonary DPI formulation are: dosage form, route of administration and important attributes of this route, dosage type, pharmacokinetics, packaging and stability requirements. Considering that the drug is poorly water soluble, a solubilising excipient is desirable to be incorporated in the formulation. For chemotactic purposes and with the aim of potentially targeting AmB towards macrophages (Chono, Tanino, Seki, & Morimoto, 2006), a carbohydrate excipient such as raffinose or mannose was employed. To improve flow properties, leucine was incorporated (Lamy et al., 2019). In order to establish the TPP, various CQAs were identified as critical, such as the yield of the manufacturing process (spray drying), AmB loading, encapsulation efficiency, geometric and aerodynamic particle size and degree of crystallinity (DC) (Guebitz et al., 2012; Walsh et al., 2018).

2.2.1.2. *Preliminary screening studies*. A seven-factor eight-run Taguchi design ( $\text{L}_2^7$ ) was employed for factor screening in order to identify the formulation and process variables that critically influence the product quality. To select the most influential variables, an Ishikawa fish-bone diagram (Fig. S1, Supplementary material) was designed to structure the risk operation for determining the causes and sub-causes affecting the CQAs.

The software Design Expert® version 10.0 (M/s Stat-Ease, Minneapolis, USA) was used to develop polynomial models which were analysed to outline the main effects for each CQA through Pareto charts (Guebitz et al., 2012). Seven factors and two levels of each factor affecting the development of the AmB DPI formulation were selected (Table S1, Supplementary material) (Guebitz et al., 2012). Five factors

were numerical (i–v) and two categorical (vi–vii):

- i) Gas flow rate: 500 or 800 (NL/h);
- ii) Aspirator settings: 85 or 100 %;
- iii) Solution feed rate: 5 or 15 %; equivalent to 2 or 6 ml/min;
- iv) Inlet temperature: 130 or 175 °C;
- v) AmB concentration in the sprayed solution: 0.0625 or 0.125 %;
- vi) Type of solubilising excipient:  $\gamma$ -Cyclodextrin ( $\gamma$ -CD) or Sodium Deoxycholate (DOC);
- vii) Type of carbohydrate excipient acting as chemotactic agent: raffinose or mannose.

A total of eight formulations were prepared.  $\gamma$ -CD and DOC were selected as their ability to solubilise AmB in aqueous media has been demonstrated (Fernandez-Garcia et al., 2017). Based on previous studies, a weight ratio of 1:100 AmB:  $\gamma$ -CD (W:W) was required to solubilise the drug (Ruiz et al., 2014). For this reason, the maximum AmB concentration selected was 0.125 %. The same concentration was used for DOC. The concentration of the carbohydrate excipient (raffinose or mannose) was fixed to be the same as that of AmB.

The solution for spray drying was prepared as follows: the solubilizing excipient (6.25 or 12.5 g) was dispersed in 200 ml of deionized water and AmB (0.125 or 0.250 g) was added to the aqueous solution. A 2 N aqueous solution of NaOH (5 ml) was required to adjust the pH to 12. Once the drug was homogeneously dissolved, H<sub>3</sub>PO<sub>4</sub> (diluted in water at 27 %) was added until a physiological pH of 7.4 was reached. In the final step, the carbohydrate excipient (0.125 or 0.25 g) was solubilized. The solution was mixed in a magnetic stirrer for 10 min until it was visually homogeneous (Ruiz et al., 2014; Salzano et al., 2017).

The final aqueous solution was spray dried in a Büchi B191 Mini Spray Dryer (Büchi Labortechnik AG, Switzerland) using a high-efficiency cyclone in an open mode. The process parameters were as follows: 130–175 °C inlet temperature, 2 or 6 ml/min solution feed rate (5 or 15 %), 500 or 800 NL/h nitrogen flow rate and 85 or 100 % aspirator force.

Once the aqueous solution was spray dried, the particles were collected inside the collection vessel and the following five responses were evaluated: yield, AmB loading efficiency, water residual content, geometric particle size and DC.

The yield was calculated taking into account the difference in weight between the dry powder collected after the spray drying process and the total weight of excipients and API introduced into the feed solution, using equation (1).

$$\text{Yield}(\%) = \frac{\text{Weight of collected spray dried formulation} * 100}{\text{Initial mass of API + excipients}} \quad (1)$$

For AmB loading efficiency (LE) quantification, a known amount of powder formulation ( $\approx 10$  mg) of each formulation of the DoE was weighed, dispersed in water (100 ml), diluted in methanol (1/10) and analysed by high performance liquid chromatography (HPLC) using an Alliance HPLC with Waters 2695 Separations module system and Waters 2996 photodiode array detector. The mobile phase consisted of 52 % HPLC grade acetonitrile, 43.7 % deionized water and 4.3 % acetic acid glacial. The mobile phase was degassed and filtered using a 0.45  $\mu\text{m}$  polypropylene Whatman® filter. Separation was performed on a Thermo Hypersil BDS C18 reverse-phase column with a length of 200 mm, an internal diameter of 4.6 mm and a particle size of 5  $\mu\text{m}$ . Samples were analyzed by UV detection at a wavelength of 406 nm. An injection volume of 100  $\mu\text{l}$  was used. The elution was carried out isocratically with a flow rate of 1 ml/min. Empower Software v3 was used for peak evaluation (Serrano et al., 2015).

The DC was calculated by Powder X-Ray Diffraction which was performed using a wide angle Miniflex II Rigaku™ diffractometer with Ni-filtered Cu K $\alpha$  radiation (1.54 Å). The tube voltage and tube current used were 30 kV and 15 mA, respectively. The PXRD patterns were recorded (n = 3) for 2 thetas ranging from 5° to 40° at a step scan rate of

0.05°/second. The percentage of crystallinity was calculated by comparing the intensity of the Bragg peaks at 13.55 and 14.5, 2  $\theta$  of the PXRD spectrum of each formulation against AmB raw material (which was considered as 100 % crystalline). Rigaku Peak Integral software was used to determine peak intensity for each sample using the Sonneveld-Visser background edit procedure. Equation (2) was used to determine DC (%):

$$\text{DC}(\%) = \frac{\text{Peak Area of the spray dried formulation} * \left(\frac{\text{LE}}{100}\right)}{\text{Peak Area of AmB raw}} \quad (2)$$

The residual water content was analyzed by Thermogravimetric Analysis (TGA) performed using a Mettler TG 50 module (Greifensee, Switzerland). Samples were placed in open aluminum pans (3–5 mg) and analyzed at a constant heating rate of 10 °C/min between a temperature range of 25 °C and 250 °C (Serrano et al., 2016b).

The geometric particle size distribution was determined by laser diffraction using a Malvern® Mastersizer 2000 (Malvern Instruments Ltd., Worcestershire, UK). AmB- DPI powder formulations were dispersed using a Scirocco dry feeder instrument with 3 bar pressure and a vibration feed rate of 75 % to get an obscuration of 0.5–3 %. The results were reported as the median particle size (D<sub>50</sub>).

**2.2.1.3. QbD-based formulations optimization studies.** Based on the preliminary studies, the critical excipient attributes affecting the spray drying process were identified. A Box Behnken experimental design was employed for systematic optimization using Design Expert® software (Table S2, Supplementary material) (Guebitz et al., 2012). The central point (0, 0, 0) was studied in quintuplicate. Three factors and three levels of each factor affecting the final DPI formulation responses were selected: i) AmB: CD weight ratio (1, 50.5 and 100), ii) AmB: mannose weight ratio (0.2, 0.6 and 1) and iii) the amount of leucine used to improve the flow properties (5 %, 10 %, and 15 %). The spray drying parameters were kept constant, as follows: 10 % (4 ml/min) solution feed rate, 742 NL/h nitrogen flow rate, 150 °C inlet temperature and 90 % aspirator rate. Regarding the formulation parameters, after the preliminary screening, the following were kept constant: i) CD as solubilizing excipient instead of DOC, considering that the latter can be more irritant to the RT and ii) mannose as chemotactic carbohydrate excipient as its efficacy has been demonstrated due to the presence of mannose receptors on the surface of macrophages (Cutler, 1998). Seven responses were evaluated: DC, LE, residual water content, yield, mass median aerodynamic diameter (MMAD), fine particle fractions (FPF) < 3  $\mu\text{m}$  and (FPF) < 5  $\mu\text{m}$ . Table S2, (Supplementary material) summarizes the experimental design matrix of the seventeen experimental runs and their factor combinations and responses.

**2.2.1.4. Optimisation of AmB DPI formulations and validation studies.** Mathematical modelling was carried out by multiple linear regression analysis (MLRA). The polynomial equations were based on the statistically significant coefficients (p < 0.05). Correlation coefficient (R<sup>2</sup>) and predicted residual sum of squares (PRESS) were used to evaluate the models. Response surface analysis was carried out employing 2D and 3D plots to understand the relationship among the different factors and the responses. The prediction of the optimum formulations was carried out by numerical optimization and desirability function. Two optimised formulations (F1 and F2) were developed with good flow properties and the DC of the drug switching from amorphous (F2) to crystalline (F1). Validation of the QbD methodology was achieved by comparing the predicted responses with the experimental ones with linear correlation and residual plots as support (Guebitz et al., 2012).

## 2.2.2. Physicochemical characterization of the optimised formulations

**2.2.2.1. Scanning electron microscopy (SEM).** The surface morphology of DPIs formulations, previously coated with gold/palladium, was

evaluated by scanning electron microscopy (SEM) using a Zeiss Supra Variable Pressure Field Emission Scanning Electron Microscope (Germany) equipped with a secondary electron detector at 5 KV (Dickinson et al., 2001).

**2.2.2.2. Fourier transforms infrared spectroscopy (FTIR).** Measurements were carried out with a PerkinElmer Spectrum 1 FT-IR Spectrometer equipped with a UATR and a ZnSe crystal accessory. Infrared spectra were scanned in the range of 650–400  $\text{cm}^{-1}$  with a resolution of 4  $\text{cm}^{-1}$ . Data was evaluated using Spectrum V.5.0.1 software. Four scans of each sample were taken (Rojek & Wesolowski, 2019).

**2.2.2.3. Modulated temperature DSC (MTDSC).** Optimised DPI powders ( $n = 3$ ) were weighed (4–6 mg) in aluminum pans with one pin-hole. MTDSC scans of the samples were recorded on a QA-200 TA instrument (TA instruments, Elstree, United Kingdom) calorimeter using nitrogen as the purge gas. A scanning rate of 5  $^{\circ}\text{C}/\text{min}$ , an amplitude of modulation of 0.796  $^{\circ}\text{C}$  and a modulation frequency of 1/60 Hz were employed (Serrano et al., 2019). The temperature range was from 10 to 210  $^{\circ}\text{C}$  (Rolon et al., 2017). Calibration of the instrument was carried out using indium as standard (Serrano et al., 2016b).

**2.2.2.4. Dynamic vapour sorption (DVS).** Vapour sorption experiments were carried out on a DVS Advantage-1 automated gravimetric sorption analyzer (Surface Measurement Systems, Alpertun, UK) at  $25.0 \pm 0.1$   $^{\circ}\text{C}$ . Water was used as the probe vapor. A mass of 15–20 mg of powder was loaded on to the sample basket. Samples were dried at 0 % relative humidity (RH) for 1 h and then subjected to step changes of 10 % RH up to 90 % RH, and the reverse for desorption. The sample mass was allowed to reach equilibrium, defined as  $\text{dm}/\text{dt} \leq 0.002$  mg/min over 10 min before the RH was changed (Curtin et al., 2013; Grossjohann et al., 2015). Two cycles of sorption and desorption were performed for each sample, after which samples were recovered and analyzed by PXRD.

**2.2.2.5. Surface area.** To determine the specific surface area by the Brunauer, Emmett, Teller (BET) isotherm method, a Micromeritics Gemini VI (Micromeritics, Norcross, GA, USA) surface area analyzer was used. The specific surface area of the samples was determined by the  $\text{N}_2$  adsorption BET multipoint method, with 6 points in the relative pressure range of 0.05–0.3 mm Hg. Each average result was calculated on the basis of three measurements (Grossjohann et al., 2015). Samples were prepared by purging under  $\text{N}_2$  overnight at 25  $^{\circ}\text{C}$ .

**2.2.2.6. Mass median aerodynamic diameter (MMAD) and fine particle fraction (FPF).** MMAD and FPF were assessed to determine the *in vitro* lung deposition of the optimized DPI AmB formulations. In accordance with the specifications for apparatus E of the European Pharmacopoeia 9.0 - Preparations for Inhalation: testing was performed using a Next Generation Impactor™ (NGI™, MSP Corporation, Shoreview, MN). The NGI™ was equipped with a stainless-steel induction port (throat adaptor) attachment and seven stainless steel compartments (stages) and one Micro-Orifice Collector (MOC) kept in a support tray. A filter paper (Whatmann™ n°1) wetted with 1 ml of acetonitrile: water (1:1, V: V) mixture was placed in each stage to facilitate sample collection and avoid particle bouncing. Aerodynamic cut off diameters (ECD) for each impactor stage at 60 L/min were calibrated by the manufacturer and stated to be: 8.06  $\mu\text{m}$ , 4.46  $\mu\text{m}$ , 2.82  $\mu\text{m}$ , 1.66  $\mu\text{m}$ , 0.94  $\mu\text{m}$ , 0.55  $\mu\text{m}$  and 0.34  $\mu\text{m}$  for stage 1 to stage 7 respectively (Park et al., 2013).

The NGI™ was coupled with a Copley TPK 2000 critical flow controller, which was connected to a Copley HCP5 vacuum pump (Copley Scientific, United Kingdom). To achieve a constant airflow rate (Q) through the system, the volumetric flow output (Qout) should be  $\pm 5$  % which was measured using a flowmeter and adjusted prior to each

experiment. Qout can be also calculated by the ideal gas law (Eq. (3)) (Park et al., 2013).

$$Q_{out} = \frac{Q_{inx} \times P_o}{P_o \times \Delta P} \quad (3)$$

Once the airflow was set at 60 L/min, the flowmeter connected to the mouthpiece was replaced by the inhaler device and the pressures were checked to verify that:  $P_3/P_2 \leq 0.5$  and  $P_1 \geq 4$  Kpa.

AmB DPI formulations and Ambisome® powder (25 mg) were weighed and loaded into size 3 hard gelatin capsules, which were individually placed in a Handihaler® device (Boehringer Ingelheim) and connected to the NGI mouthpiece via a custom-made mouthpiece adapter Copley Scientific, United Kingdom). The capsule content was released by being needle-pierced opened by the Handihaler® and the system was vacuumed to produce air streams of 60 L/min for 4 s. The collecting solvent used was acetonitrile:  $\text{H}_2\text{O}$ , 1:1 (v/v). The collected samples were diluted as appropriate and analyzed by HPLC as previously described (Corrigan et al., 2006).

The emitted dose of one capsule (i.e. the percentage of emitted AmB), was determined from the various depositions in the NGI, from the first to the last stage, excluding the amount remaining in the device. The MMAD and the FPF < 5  $\mu\text{m}$  and < 3  $\mu\text{m}$  were calculated based on the AmB deposited fraction on each NGI stage, as previously described (Corrigan et al., 2006). All the experiments were performed in triplicate.

In further studies, *in vitro* lung deposition of optimised AmB DPI formulations was studied at different flow rates simulating a reduced inspiration breath characteristic in patients suffering from pulmonary infections: 30 L/min for 8 s as a DPI and nebulization at 25 L/min for 15 min for formulations dispersed in 5 ml of  $\text{H}_2\text{O}$  (at 5 mg/ml) using a NB-810B ultrasonic mesh nebulizer (140 KHz and 0.3 ml/min nebulization rate).

### 2.2.3. Investigation of fixed-dose combination DPI containing AmB and salbutamol sulfate (SS)

A salbutamol sulfate (SS)–AmB fixed-dose formulation was developed as a combination to treat fungal pulmonary infections which are commonly associated with low breathing capacity (Ader et al., 2005). The SS-AmB DPI formulation was prepared following the same manufacturing method as for the F2 optimised formulation which will be later described in the result Section 3.1. Briefly, in this fixed-dose combination, 39.7 % AmB was formulated with 0.8 % SS, 39.7 %  $\gamma$ -cyclodextrin, 7.3 % mannose and 12.5 % leucine. The rationale behind this combination is that in the final capsule intended for inhalation as a DPI (with a total weight of 25 mg), the amount of AmB and SS is 10 mg and 200  $\mu\text{g}$  respectively which is equivalent to the current dose utilized in the treatment of bronchospasm (Broeders et al., 2005).

The fixed-dose SS-AmB DPI formulation was characterised by scanning electron microscopy (SEM) and aerodynamic flow properties (MMAD and FPF < 5  $\mu\text{m}$  and FPF < 3  $\mu\text{m}$ ) by NGI™ following the same method previously described in Section 2.2.2.

### 2.2.4. In vitro release studies

*In vitro* release studies were performed on F1 and F2 optimised AmB DPI powder formulations and compared to unprocessed AmB. Formulations were weighed (a mass equivalent to 5 mg of AmB) and diluted with 2 ml of Hanks Buffered Salt Solution (HBBS), which is a simulated epithelial lining fluid (ELF), consisting of potassium chloride (7 mg/ml), potassium phosphate monobasic (400 mg/ml), sodium bicarbonate (60 mg/ml), sodium chloride (350 mg/ml), sodium phosphate dibasic (8 g/ml), D-glucose (dextrose) (48 mg/ml) adjusted to pH 7.4 in  $\text{H}_2\text{O}$  (Tewes et al., 2016). Dispersed formulations were filled inside dialysis membranes in which 0.5 mm glass beads were added to avoid floating. Filled dialysis bags were introduced into 100 ml of HBBS and maintained at 37  $^{\circ}\text{C}$  in a bath with constant shaking. Samples (1 ml) were withdrawn at different time points: 30, 60, 120, 180, 240, 300, 360 min and 20 and 24 h. Media was replaced with fresh buffer at each sampling time point.

Samples were centrifuged at 5000 rpm and the supernatant was analysed by HPLC using the method described above. The assay was performed in triplicate.

### 2.2.5. *In vitro* antimicrobial activity-disk diffusion halo assay

The antifungal activity of the optimised AmB DPI formulations was tested against three different strains of *Candida* (*Candida albicans*; CECT 1394, *Candida glabrata* 60750 and *Candida parapsilosis* 57744). These three species have been selected due to their higher incidence rate and prevalence compared to other *Candida* sp. Antifungal activity was tested by an agar diffusion assay, according to the European Pharmacopoeia 8.0 and as previously described by Ruiz et al. (Ruiz et al., 2014). Prior to the beginning of the study, yeast isolates were cultured in Sabouraud dextrose agar at 30 °C for 72 h to ensure viability and absence of contamination. Antifungal sensibility was assayed in Müeller Hinton agar (MHA) supplemented with glucose (2 % w/w) and 0.5 µg/mL methylene blue. The MHA (200 ml) was sterilized at 121 °C and once attemperated, 3 ml of yeast suspension, prepared in sterile saline (NaCl 0.9 %) and adjusted to 0.1 Abs at 600 nm, was inoculated. The MHA with the inoculated *Candida* was placed onto Petri dishes (Serrano et al., 2015). Optimised AmB-DPI formulations (F1 and F2) were weighed and dispersed in deionized water resulting in a final AmB concentration of 500 µg/ml. As a control, AmB dissolved in dimethyl sulfoxide (DMSO) at the same concentration and AmB NeoSensitab® disks (containing 10 µg of AmB) were used. Paper disks (6 mm) were embedded with 20 µl of each sample. The amount of drug inoculated per disk was 10 µg (which is equivalent to the amount of AmB contained in each NeoSensitab® disk). Once the disks were dried and the agar solidified, the disks were placed onto the inoculated agar plates. The plates were kept at 5 °C for 2 h followed by 48 h at 30 °C and then the diameter of the growth inhibition halos was measured. The study was performed in triplicate.

### 2.2.6. *Ex-vivo* red blood cell (RBC) haemolytic studies

Venous blood was obtained from a healthy volunteer and collected into an EDTA-coated Vacutainer tube to prevent coagulation. The blood was centrifuged at 1000 rpm for 5 min and the haematocrit and plasma levels were marked on the tube. The supernatant was discarded. The tube was filled to the plasma level marked line with 150 mM NaCl solution and the tube was gently mixed. The tube was centrifuged (5 min at 1000 rpm) and the supernatant was discarded again. The RBCs were washed twice with 150 mM NaCl solution as previously described. After the last wash, the supernatant was discarded, and the RBCs were diluted with PBS at pH 7.4 to 4 % final concentration ( $4.81 \times 10^5$  RBC/ml). The diluted RBCs were then added into a 96 well plate (180 µl/well) (Serrano et al., 2013). Two types of experiments were performed, in triplicate as below described.

In the first set of experiments, the aim was to evaluate the haemolytic effect of the optimized AmB-DPI formulations. Stock solutions of the optimised AmB DPI formulations (1 mg/ml) were prepared. As a comparison, a standard solution of AmB in DMSO at the same concentration was prepared. Formulations were diluted using deionised water at different concentrations (250–3.9 µg/ml) and 20 µl of each sample concentration were loaded into the wells. As a positive control, a 20 % solution of Triton X-100 (20 µl) was added. As a negative control, PBS pH 7.4 (20 µl) was incorporated. Plates were incubated at 37 °C for 1 h. Subsequently, plates were centrifuged at 2500 rpm for 5 min to pellet intact erythrocytes. Supernatants (50 µl) were transferred into a clear, flat-bottomed 96-well plate. The absorbance of the supernatants was measured using a plate reader (BioTek, ELx808) at 595 nm. The percentage of haemolysis was calculated using the following equation:

$$\text{Haemolysis (\%)} = \frac{ABS_{\text{sample}} - ABS_{\text{PBS}}}{ABS_{\text{Triton}} - ABS_{\text{PBS}}} \times 100 \quad (4)$$

where  $ABS_{\text{PBS}}$  is the average of the absorbance from the negative control and the  $ABS_{\text{Triton}}$  is the average of the absorbance from the positive control. The concentration of AmB-DPI formulation that

produces 50 % haemolysis at the tested concentration ( $HC_{50}$ ) was calculated using Compusyn™ software.

In the second set of experiments, the aim was to investigate the effect of leucine and mannose on the different AmB aggregate states. AmB in water, and depending on the excipients, can be found in a monomeric state or aggregated, forming oligoaggregates (known as dimers) or polyaggregates (Fernandez-Garcia et al., 2017). The second haemolytic study was performed using the same method as described above in order to determine any protective effect of leucine or mannose incorporated in AmB DPI formulations when tested against red blood cells. An equilibrium between the dimeric and monomeric forms was found in the AmB DPI formulations. Dimeric and monomeric AmB solutions were prepared using AmB:DOC (50:41, w:w ratio) and AmB:CD (1:100, w:w ratio) respectively, as previously described (Serrano et al., 2013). Leucine and mannose were dissolved in water. Each of the compounds was tested separately with dimeric or monomeric AmB solutions at a weight ratio of 1:1. In addition, mannose and leucine were tested together at the weight ratio 0.5:0.5:1 (mannose:leucine:AmB) with each of the aggregation states of AmB.

### 2.2.7. *In vitro* activity against *Leishmania*

The optimised AmB DPI formulations and unprocessed AmB were tested at different concentrations (100 µg/ml to 0.19 µg/ml) against *Leishmania donovani* and *Leishmania infantum* promastigotes (provided from Centro Nacional de Microbiología of the Instituto de Salud Carlos III (Madrid- Spain) (Bilbao-Ramos et al., 2012; Dea-Ayuela et al., 2009). Parasites were cultured in Schneider's insect medium at 26 °C and supplemented with heat-inactivated foetal bovine serum, penicillin, and streptomycin at a concentration of 100 IU/ml and 100 µg/ml, respectively. Log-phase promastigotes were cultured in 96-well plates and  $2.5 \times 10^6$  parasites were added per well (100 µl). F1 and F2 DPI formulations were dissolved in deionised water at different concentrations (100 µg/ml to 0.19 µg/ml) and were also added to the wells (100 µl). After 48 h of incubation at 26 °C, a resazurin solution (20 µl, 2.5 mM) was added to each well and, 3 h later, the fluorescence intensity (535 nm excitation wavelength, 590 nm emission wavelength) was measured using a Tecan® Infinite 200 fluorimeter. The efficacy of each formulation was estimated by calculating the  $IC_{50}$  (concentration needed to kill 50 % of the parasites) by Probit analysis using Minitab (Coventry, UK) (Bilbao-Ramos et al., 2012).

### 2.2.8. Cytotoxicity study

The *in vitro* cytotoxicity studies were carried out in a J774 murine macrophage cell line. The macrophages were maintained in RPMI-1640 supplemented medium with 10 % heat-inactivated foetal bovine serum (FBS) (30 min at 56 °C), 100 U/mL of penicillin G and 100 µg/mL streptomycin. Macrophages were detached from the flasks using 0.03 % EDTA-0.05 % Trypsin in PBS and were incubated in a 96 well plate at 37 °C and 5 % CO<sub>2</sub> humidity chamber afterwards. Macrophages were placed in 96-well plates ( $5 \times 10^4$  cells/well) with 100 µl of RPMI-1640 medium and incubated for 24 h at 30 °C, 5 % CO<sub>2</sub>. Later, medium was discarded and replaced with 200 µl of formulation and incubated again for 24 h. Optimised AmB DPI formulations, F1 and F2 and unprocessed AmB were tested at different concentrations in each well (250 µg/ml to 0.078 µg/ml) in triplicate. After the 24 h incubation period, resazurin (20 µl, 1 mM) was added and the plates were incubated for another 3 h. Then, the fluorescence intensity was measured (535 nm excitation wavelength, 590 nm emission wavelength) (Bilbao-Ramos et al., 2012; Smith et al., 2018). The cytotoxicity of each formulation was estimated by calculating the  $CC_{50}$  (concentration needed to kill 50 % of the macrophages) by Probit analysis. The selectivity index (SI) was calculated as expressed in Equation (5) (Smith et al., 2018):

$$SI = \frac{CC_{50}}{IC_{50}} \quad (5)$$

### 2.2.9. Macrophages uptake assay

J774 cell lines (murine monocyte-like cell line) were grown in Minimum Essential Medium Eagle supplemented with FBS, 100 UI/mL of penicillin G and 100 µg/mL streptomycin in 25 ml flasks at 37 °C and a humidified 5 % CO<sub>2</sub>/air atmosphere. The J77A cells (100 µl equivalent to 5 × 10<sup>5</sup> cell/ml) were incubated at 37 °C with 100 µl of each of the optimised AmB DPI formulations after being reconstituted with deionized water and diluted at different concentrations (25–0.195 µg/ml). Dimeric AmB, prepared as described above, was tested as a control at the same concentrations. After several incubation times (1, 4 and 24 h), the supernatant was discarded, and all the plate was washed with cold macrophage medium (RPMI). The cellular lysis was performed with 250 µl of Triton 1 % in PBS followed by 30 min under mild stirring. Afterwards, 100 µl were transferred to another 96 well plate and 100 µl of MeOH was incorporated to solubilize the AmB and precipitate the cell debris (Chono et al., 2006). The plate was centrifuged for 10 min at 2500 rpm. After that, the supernatant was collected and analyzed by HPLC as above described.

### 2.2.10. Pharmacokinetic studies

All experiments were performed in the INSERM U1070 laboratory at the University of Poitiers using rats OFA 250/275gr bought from Charles River (production area B7). Animal work was carried out in accordance with the Principles of Laboratory Animal Care (26a) and with EC Directive 2010/63/EU. They were approved by the local ethics committee (COMETHEA) and registered by the French Ministry of Higher Education and Research (n°2015042117101247). Animals were acclimatized in wire cages in a 12-h light–dark cycle for a minimum of 5 days before the beginning of the experiment. During this period, they had free access to food and water. They were randomly split into three groups (n = 21).

In the first group (G1) Ambisome® (purchased from Gilead Sciences S.L.) was intravenously administered at 5 mg/kg. Group 2 (G2) and Group 3 (G3) received F1 and F2 optimised AmB DPI formulations intratracheally administered using a MicroSprayer IA-1B system (Penn Century Inc, Philadelphia, USA). Animals received a dose equivalent to 5 mg/kg of AmB. Previous to drug administration, isoflurane (3 % air at 550 ml/min) was administered to all the rats for a short sedation period. Rats were maintained by the upper incisors on a rodent work stand inclined at an angle of 45° (Tem, Lormont, France). Vocal cords were visualized with the help of an otoscope. The tube of the MicroSprayer IA-1B system was inserted between the vocal cords, and the AmB DPI formulations were nebulized into the lung. Rats were still asleep approximately during 5 min post-dosing. Arterial blood was collected at 1, 3, 6, 18, 30, 48 and 72 h post-administration via intracardiac puncture. Plasma was separated by centrifugation (1,000 g, 15 min) and frozen at –80 °C until analysis. Bronchoalveolar lavage (BAL) fluid collection was performed at the same times by instilling a catheter at 50 mm depth into the trachea. The highest possible volume was collected in order to estimate epithelial lining fluid (ELF) drug concentration. BAL fluid was centrifuged (1,000 g, 15 min) and AmB was quantified. AmB concentration was analyzed by liquid chromatography-tandem mass spectrometry (LC-MS/MS) validated method under ISO 9001 certification. Intraday and between-day variability were characterized with a precision and bias of < 20 %. Concentrations of ELF were calculated using the urea dilution method (Lamy et al., 2018).

### 2.2.11. Stability studies

**2.2.11.1. Accelerated stability studies.** The optimised AmB DPI formulations and unprocessed AmB (≈5 mg) were placed in uncapped HPLC vials and introduced into test chambers where they were exposed to different conditions of temperature and humidity: 40/65, 50/85, 50/10, 60/30, 60/65, 70/10 (°C/ % RH). The relevant humidity capsules (Amebis Ltd, Dublin, Ireland) were introduced in the stability chambers

which were put inside ovens at the selected temperature in order to ensure that the RH equilibrium was reached prior to aging of the formulations. A sensor cap with a data logger on it was used to seal the test chamber, and to collect and transmit the temperature and humidity test conditions to the Amebis Control Software. Amebis Software was used to calculate the mean kinetic temperature and relative humidity for every condition. Samples were collected and analysed by the HPLC method previously described for chemical degradation at different time points (1, 3, 6 and 14 days). The stability modelling was performed using ASAPprime® software. The effect of temperature and RH on degradation rates was estimated by a humidity-corrected Arrhenius equation (Serrano et al., 2018; Waterman, Swanson, & Lippold, 2014) (Eq. (3)):

$$\ln K = \ln A - \frac{E_a}{RT} + B(RH) \quad (6)$$

Where K is the degradation constant (% AmB/day), A is the collision frequency, E<sub>a</sub> is the activation energy, B is the humidity sensitivity factor, T is the absolute temperature and R is the gas constant. The method used was “potency with RH” based on the amount remaining of AmB, at different time points, dependant on variations in temperature and RH. The parameter selected for modelling was 2500 Monte Carlo simulations and 90 % specification limit. Different fitting methods were assessed: Avrami, diffusion, first order, second order and zero order. The one with the highest R<sup>2</sup> was selected for shelf-life prediction at the following conditions of temperature (°C) and relative humidity (RH): 25/60, 25/10, 4/10.

**2.2.11.2. Long term stability studies.** F1 and F2 and the unprocessed AmB were placed in uncapped HPLC vials and introduced in stability chambers at ICH conditions (25 °C, 60 % RH; 25 °C, 10 % RH and 4 °C, 10 % RH). The samples were analysed by HPLC to determine the AmB potency (%) in the formulation at different times (3, 12 and 24 months) (Serrano et al., 2015). The estimated shelf-life values were compared to those obtained from experimental data.

### 2.2.12. Statistical analysis

Statistical analysis was performed via one-way ANOVA test using Minitab 17 (Minitab Ltd, Coventry, UK) followed by Tukey's test considering p-values for statistical significance < 0.05 (Serrano et al., 2016a).

## 3. Results

### 3.1. Preliminary screening

A Taguchi design was employed to perform the screening of several process and formulation parameters, in total seven factors at two levels each. This design has the specific advantage of requiring a minimal number of experimental runs (n = 8) including a large number of independent variables (Table S1, Supplementary material) (Shukla, Mishra, Bhoop, & Katare, 2015).

Pareto charts showed that the variables/responses that were most subject to change during the spray drying process were yield and particle size (represented by D<sub>50</sub>). All the formulations exhibited a particle size between 1 and 5 µm. The higher the gas flow rate, the lower was the median geometric particle size, D<sub>50</sub>. Regarding the solubilising excipient, the greater the amount of DOC, the lower was the particle size and the yield. The aspirator setting and inlet temperature had opposite effects on the yield. A higher yield was obtained at lower aspirator rates and higher inlet temperatures. Based on these results, the gas flow rate and inlet temperature were fixed at 742 NL/h and 150 °C respectively while a 90 % aspirator setting was selected for the second DoE (Box-Behnken). No statistically significant differences were observed for the DC and the spray drying rate in the Taguchi DoE. To avoid clogging of the nozzle, a 10 % solution feed rate (equivalent to 4 ml/min) was selected for further studies.

In the second DOE, the effect of three factors (weight ratio of CD: AmB, weight ratio of mannose:AmB and percentage of leucine) at three levels was investigated in more detail. CD was chosen as the solubilising excipient instead of DOC due to the fact that the DOC may be more irritant to the lung than CD (Cutler, 1998), and also because the use of CD led to higher yield and loading efficiency in the preliminary screening studies. The three levels of AmB: CD evaluated were 1:1, 1:50 and 1:100 (w:w). Even though, no significant differences were found between the use of raffinose and mannose in the preliminary screening studies, the latter was selected as its efficacy as chemotactic agent for macrophages has been previously demonstrated (Cutler, 1998; Suzuki et al., 2018) and this could potentially be beneficial in the treatment of intracellular parasites such as disseminated leishmaniasis. Three different AmB: mannose ratios were used: 1:1; 1:3 and 1:5 (w:w). The impact of leucine on the flow properties of the formulations was studied in more detail in this second DoE. The effect of three different levels, 5, 10 and 15 % of leucine, was investigated.

### 3.1.1. QbD-based model development and response surface analysis

Polynomial analysis was carried out by a multilinear regression analysis method, which indicated that the linear and two factor interaction models were the best fit for the parameters assessed, except for the yield response for which a quadratic model showed a better fit. The coefficients of the model equations generated for each CQA revealed goodness of fit of the experimental data to the selected model (with high values of  $R^2$  and low p-values < 0.05) for three of the responses: MMAD, DC and yield. No significant differences were observed in the percentage of water content and encapsulation efficiency ( $p > 0.05$ ).

The MMAD 3D-response surface plot revealed a higher influence of the amount of leucine, mannose and CD. Lower MMAD results were obtained when greater amounts of leucine, lower AmB: mannose and AmB: CD ratios were spray dried (Fig. 1a-b).

Regarding the DC, the most influential variables were the ratio between AmB and CD and mannose. A higher DC was obtained when larger amounts of mannose were used, but with lower amounts of CD and leucine, thus, 1:1 AmB:CD ratio, 5 % of leucine and 1:1 AmB: mannose ratio (Fig. 1c-d) provided the highest DC value. Similar effects were

observed for the yield (Fig. 1e-f). Yield increased significantly when 5 % leucine and 1:1 AmB: CD ratio were used in the formulation. In the case of the AmB: mannose ratio, the yield was lower at the central point but increased at the extremes (1:0.2 and 1:1).

### 3.1.2. Search for the optimum formulation and QbD validation

The search for an optimum formulation was carried out by trading-off various CQAs to attain the desired objectives, giving priority to the minimisation of the MMAD and the enhancement of the yield. Two formulations were optimised in the Box-Behnken design (denominated as F1 and F2) based on different DC values (Table S2, Supplementary material) in which the DC was maximised in F1 and minimised in F2.

Based on the aforesaid objectives, the optimised formulation parameters for F1 were: 1:1 AmB:CD weight ratio, 1:1 AmB:mannose weight ratio and 10.4 % leucine, while for F2, the optimised formulation consisted of: 1:1 AmB:CD weight ratio, 1:0.2 AmB:mannose weight ratio and 12.6 % leucine. Validation of the QbD methodology revealed close proximity between the predicted values of the responses with those observed for the prepared checkpoint formulations (Table S3 Supplementary material). The percent prediction error for the CQAs varied between 0.41 and 3.37 %, indicating excellent goodness of fit for the predictive models.

### 3.2. Physicochemical characterization

Quasi-spherical collapsed particles with rough surfaces were observed in the SEM micrographs of F1 and F2. Collapsed particles can be the result of combining high gas flow rate and low feed rate, leading to fast water evaporation. Also, rough surfaces can be attributed to the presence of deposited leucine (Lamy et al., 2019). In the F1 formulation, small, unencapsulated crystals, close to 1  $\mu\text{m}$  in size, were observed which can explain the greater DC determined for this formulation (Fig. 2a-b).

The DVS sorption profiles for both F1 and F2 formulations showed high water uptake (49.7 % and 50.7 % respectively) between 70 and 90 % relative humidity (Fig. 2c-d) which is a common behaviour for spray dried formulations. No mass loss associated with solid state changes

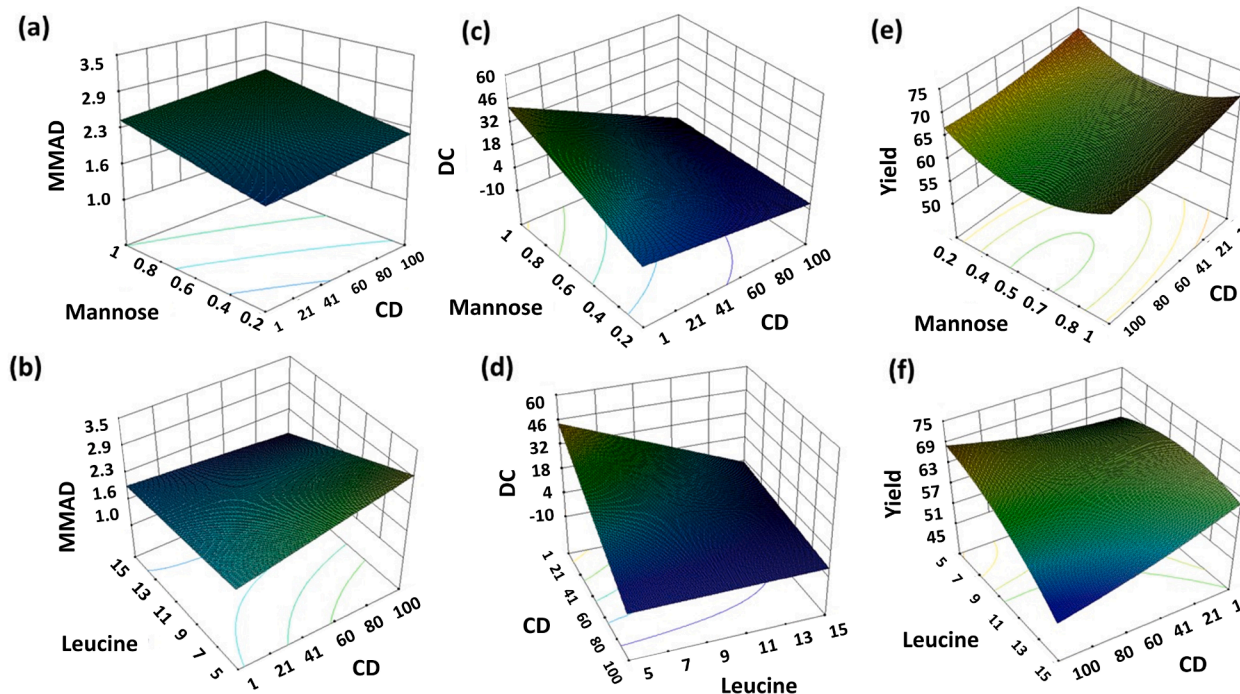
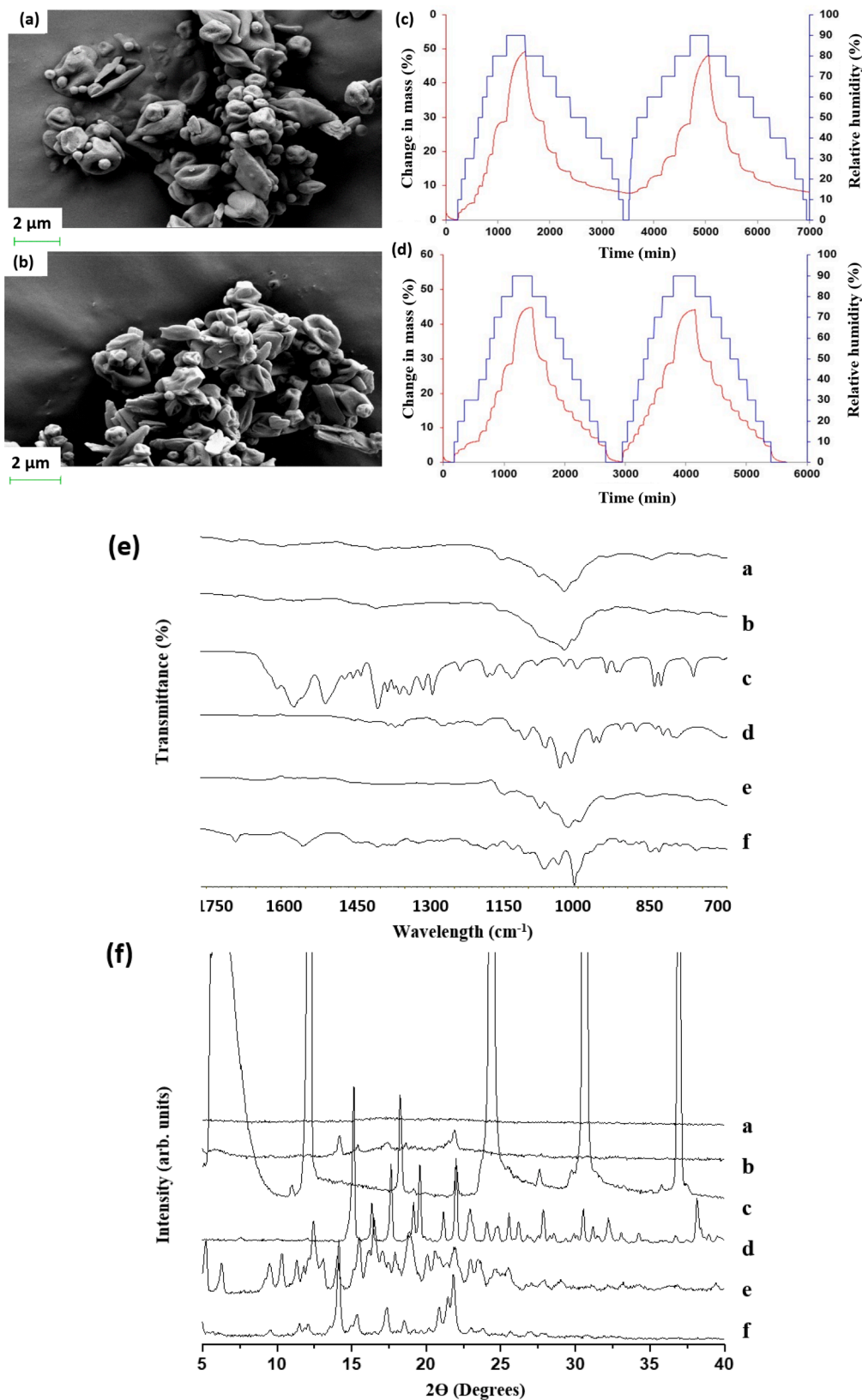


Fig. 1. 3D response surface showing the influence of the formulation excipients on the MMAD ( $\mu\text{m}$ ) (a, b), the DC (%) (c, d) and the yield (%) (e, f) respectively. Key: Leucine is expressed in %; CD is expressed as AmB:CD weight ratio (from 1 to 100, w:w) and Mannose is expressed as AmB:Mannose weight ratio (from 0.2 to 1 w:w).





**Fig. 2.** Physicochemical characterisation of F1 and F2 AmB DPIs. Key: (a) SEM of F1; (b) SEM of F2; (c) DVS profile of F1; (d) DVS profile of F2; (e) FT-IR spectra: a) F2, b) F1, c) Leucine, d) Mannose, e) CD, f) Unprocessed AmB; (f) XRD patterns: a) F2, b) F1, c) Leucine, d) Mannose, e) CD, f) Unprocessed AmB.

(such as amorphous to crystalline transition) was observed in the first or second sorption cycles for either of the formulations, indicating good physical stability.

In FT-IR, broader bands were observed for both optimised formulations due to the amorphous nature of the excipient matrix (Fig. 2e). A shift was observed in the C=O at 1691 cm<sup>-1</sup> of the AmB and the C—O stretching band at 1116–1020 cm<sup>-1</sup> of the  $\gamma$ -CD, which may be attributed to H-bond interactions between both components. This shift was more pronounced in the F2 amorphous formulation than in the semi-crystalline F1 material. PXRD diffractograms showed characteristic Bragg peaks for all unprocessed excipients and AmB raw material. After spray drying, an amorphous halo was observed only for the F2 formulation (Fig. 2f), while Bragg peaks attributed to AmB were found in the F1 formulation (Fig. 2f).

The surface area of F1 and F2 ( $5.06 \pm 0.21$  m<sup>2</sup>/g and  $4.98 \pm 0.19$  m<sup>2</sup>/g respectively) was 8-fold greater than the  $\gamma$ -CD raw material ( $0.63 \pm 0.11$  m<sup>2</sup>/g) but lower than unprocessed AmB ( $11.18 \pm 0.48$  m<sup>2</sup>/g), which can be related to the fact that AmB raw material is a micronized powder with lower geometric particle size (<3  $\mu$ m).

In the DSC thermograms, no Tg in the reversing heat flow signal was found for either of the DPI formulations, which can be explained by interference from other excipients (Fig. S2, Supplementary material). The F2 thermogram showed: i) a broader dehydration peak than F1, ii) an absence of endothermic peak of mannose at 135.8 °C which is clearly observed in the physical mixture of F2 and ii) a less pronounced dehydration peak of AmB at 94.7 °C than F1, with all three observations being associated with the difference in amorphous content between F1 and F2. AmB decomposes at temperatures above 160 °C and hence, the DC could not be quantified based on the heat of fusion.

### 3.2.1. Mass median aerodynamic diameter (MMAD) and fine particle fraction (FPF)

MMAD and FPF values for F1 and F2 DPI formulations were evaluated at two different conditions (60 L/min for 4 s and 30 L/min for 8 s). Formulations were also reconstituted in deionized water at 5 mg/ml to test lung deposition on nebulization for 15 min at 25 L/min. AmBisome®, the liposomal lyophilised intravenous formulation, was also tested as a dry powder at 60 L/min for 4 s and nebulized at 25 L/min for 15 min after being reconstituted in deionized water at the same concentration. F1 and F2 DPI formulations showed good *in vitro* deposition at 60 L/min with FPF < 5  $\mu$ m close to 80 % and a MMAD below 3  $\mu$ m (Table 1). When comparing deposition characteristics at different air flow rates, F1 showed a more consistent profile, while F2 was more sensitive to air flow changes exhibiting a significant reduction of 25 % in the FPF < 5  $\mu$ m from the DPI at 30 L/min and by nebulization at 25 L/min (Fig. 3, Figs. S3–S5 in Supplementary material). Overall, F2 showed a greater mass loss in the Handihaler and the upper parts of the respiratory tract (mouthpiece adaptor and induction port) ca. 50 % (Fig. 3). The marketed AmB parenteral formulation (AmBisome®) showed a markedly different profile when delivered via the DPI at 60 L/min compared to the reconstituted liquid nebulized at 25 L/min. In clinical practice, AmBisome® is a lyophilised powder that is reconstituted in

water and administered by nebulisation to patients. The nebulisation resulted in greater lung deposition (FPF < 5  $\mu$ m of 95 %) (Table 1). However, >30 % of the lyophilized powder formulation was retained in the Handihaler, probably because it is a formulation intended for parenteral use, and the powder has not been engineered with a view to DPI delivery (Fig. 3).

### 3.3. Fixed-dose combination DPI containing AmB and salbutamol sulfate (SS)

Using the same process and formulation parameters as were used to prepare F2, a fixed-dose combination DPI combining AmB and SS was developed to treat fungal lung infections associated with bronchoconstriction. The incorporation of SS resulted in more spherical particles with rough surfaces. The presence of unencapsulated crystals was not observed (Fig. 4). The aerodynamic performance of the formulation was excellent, with high FPF below 5 and 3  $\mu$ m (75.9 and 73.8 % respectively, from the Handihaler device at 60 L/min for 4 s), an MMAD of 2.43  $\mu$ m and a homogeneous deposition of AmB and SS (Fig. 5). The main difference observed in the deposition pattern between the two APIs was the greater percentage recovered of SS in stage 7 compared to AmB which may be advantageous bearing in mind that SS should reach the bronchi to be effective, while AmB should be distributed along the entire respiratory tract where fungal cells are located (Fig. S6 in supplementary material).

### 3.4. In vitro release studies

From 4 h onwards, the dissolution rates for AmB from the F1 and F2 formulations were 2 and 3-fold higher respectively than the unprocessed AmB. The F1 formulation exhibited a supersaturation state at earlier time points, which may be related to the easier wettability of the powder but also the combination of amorphous and crystalline domains (Fig. 5a).

### 3.5. In vitro antifungal activity

The inhibition zone diameters were measured at points where there was a complete inhibition of yeast growth. The isolates were classified as susceptible (S) to AmB when the inhibition zone was > 15 mm, resistant (R) when it was < 10 mm and intermediate (I) or susceptible-dose dependent when the inhibition zone was between 11 and 14 mm (Ruiz et al., 2014). The three strains of *Candida* tested were susceptible to the AmB released from F1 and F2 formulations, with an inhibition halo >15 mm. F1 and F2 showed a significantly higher efficacy (p < 0.05) than the commercial AmB disks (Neo-Sensitabs®) against *C. albicans* and *C. parapsilosis* (Fig. 6).

### 3.6. Ex-vivo red blood cell (RBC)-haemolysis studies

In the first study, the haemolytic activity (HC<sub>50</sub>) of AmB DPI optimised formulations, F1 and F2 was 13.9  $\mu$ g/ml and 11.3  $\mu$ g/ml

**Table 1**

FPF below 5 and 3  $\mu$ m and MMAD for F1, F2 and AmBisome® at the three different conditions: DPI at 60 L/min for 4 s, DPI at 30 L/min for 8 s and nebulization at 25 L/min for 15 min. Key: NT, not tested.

Conditions	F1			F2			AmBisome®		
	FPF < 5 $\mu$ m (%)	FPF < 3 $\mu$ m (%)	MMAD ( $\mu$ m)	FPF < 5 $\mu$ m (%)	FPF < 3 $\mu$ m (%)	MMAD ( $\mu$ m)	FPF < 5 $\mu$ m (%)	FPF < 3 $\mu$ m (%)	MMAD ( $\mu$ m)
60 L/min 4 s	81.45	67.16	1.66	79.32	53.27	2.42	4.26	0.43	4.46
SD	3.75	3.39	0.56	3.13	0.91	0.89	0.25	0.17	0.94
30 L/min for 8 s	68.95	52.47	3.48	53.98	42.12	3.28	NT	NT	NT
SD	0.91	2.78	1.23	2.32	5.07	1.42	NT	NT	NT
25 L/min for 15 min	63.84	46.06	3.85	55.11	47.13	4.14	95.80	74.38	2.50
SD	1.12	1.18	2.36	3.92	3.25	1.01	1.32	1.54	1.16

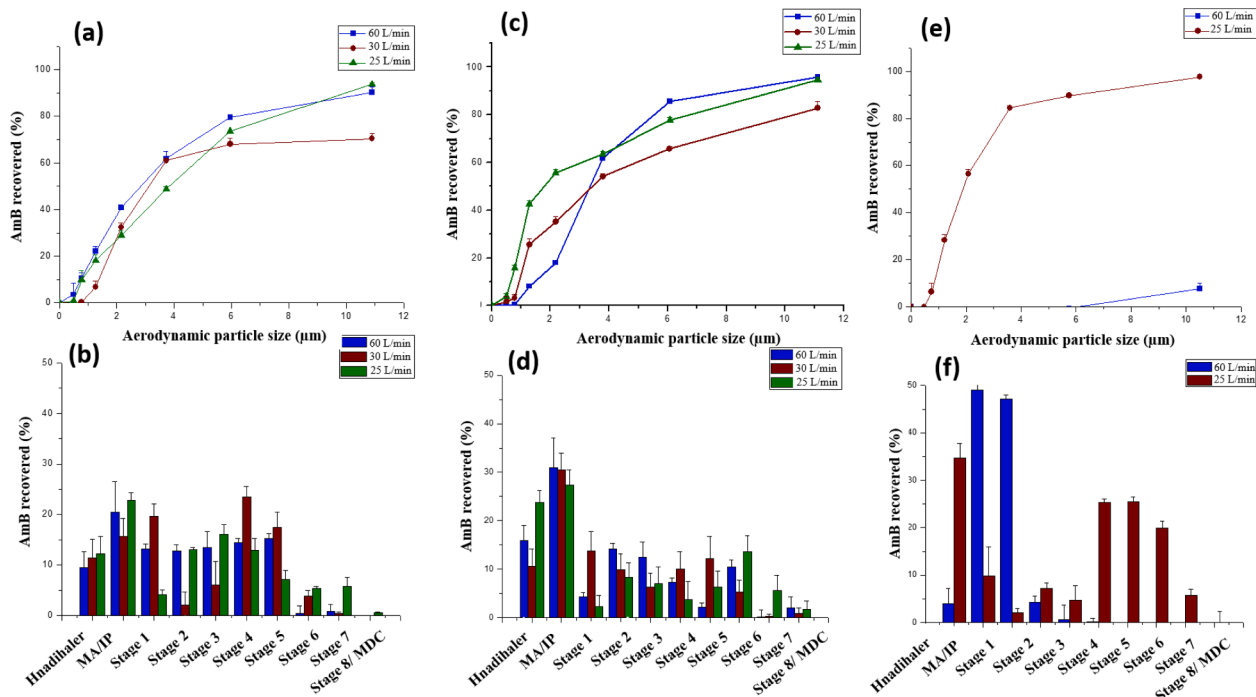


**Fig. 3.** *In vitro* deposition characteristics of F1, F2 and AmBisome® at different conditions in the NGI: dry powder using 60 L/min for 4 s, dry powder using 30 L/min for 8 s and nebulisation after reconstitution in deionized water at 25 L/min for 15 min. Key: (a) Cumulative drug deposition of F1; (b) Percentage of AmB recovered in different stages from F1; (c) Cumulative drug deposition of F2; (d) Percentage of AmB recovered in different stages from F2; (e) Cumulative drug deposition of AmBisome® at 60 L/min and 25 L/min; (f) Percentage of AmB recovered in different stages from AmBisome® tested at 60 and 25 L/min.

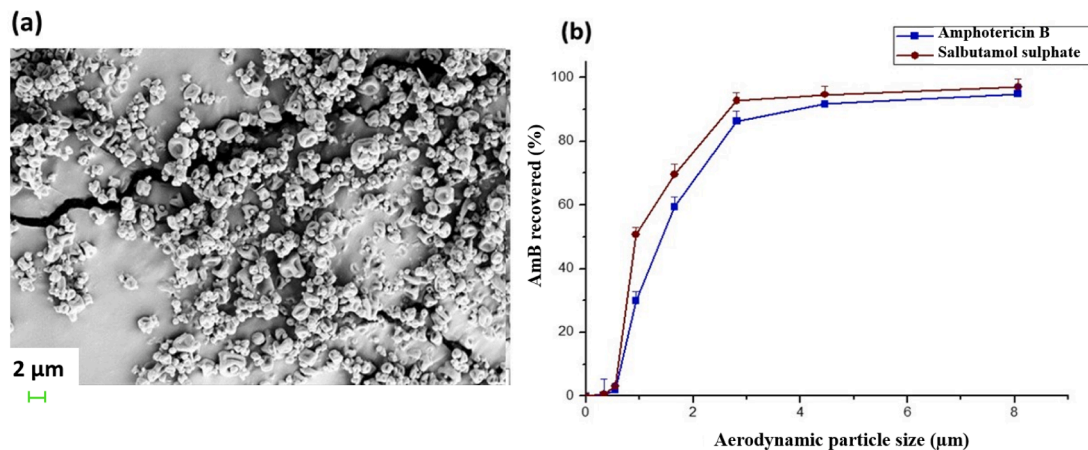


**Fig. 4.** AMB-SS DPI formulation. (a) SEM micrographs and (b) Percentage recovered of SS and AmB recovered at 60 L/min for 4 s.

respectively. Both formulations were 2 and 1.6-fold less haemolytic than AmB alone dissolved in DMSO. It is well-known that AmB is a very haemolytic drug, especially in its dimeric or monomeric states (Espada et al., 2008). The effect of the excipients (leucine and mannose) on the AmB haemolytic toxicity was studied in more detail in a second experiment. Interestingly, the second study revealed that leucine and mannose had a protective effect on red blood cells only when used in combination at a 1:1 (w:w) ratio, but not separately, both for monomeric and dimeric AmB (Fig. 7). This could explain why the F1 and F2 formulations exhibited a lower haemolytic toxicity compared to AmB dissolved in DMSO (monomeric state).

### 3.7. *In vitro* activity against *Leishmania* promastigotes and cytotoxicity against macrophages

F1 and F2 exhibited a similar activity against *Leishmania* infantum

with  $IC_{50}$  values of  $0.534 \pm 0.076 \mu\text{g/ml}$  and  $0.312 \pm 0.036 \mu\text{g/ml}$  respectively. However, F2 exhibited 3-fold greater *in vitro* activity against *Leishmania donovani* ( $IC_{50}$  of  $0.84 \pm 0.51 \mu\text{g/ml}$  versus  $2.62 \pm 0.54 \mu\text{g/ml}$  of F1). Both F1 and F2 formulations showed very low cytotoxicity against murine macrophages with a  $CC_{50}$  of  $191.30 \pm 12.38 \mu\text{g/ml}$  and  $230.23 \pm 71.85 \mu\text{g/ml}$  respectively, resulting in a very promising selectivity index against both *Leishmania* sp. (higher than 73 for F1 and higher than 273 for F2) (Table S4 Supplementary material). Further studies in amastigotes should be performed to correlate the *in vitro* activity against promastigotes.

### 3.8. Macrophages uptake studies

The *in vitro* uptake profile of AmB-DPI optimised formulations in differentiated J77A cells was markedly different from dimeric AmB. F1 exhibited a 5 and 8-fold higher uptake than F2 at 4 and 24 h ( $p < 0.05$ )

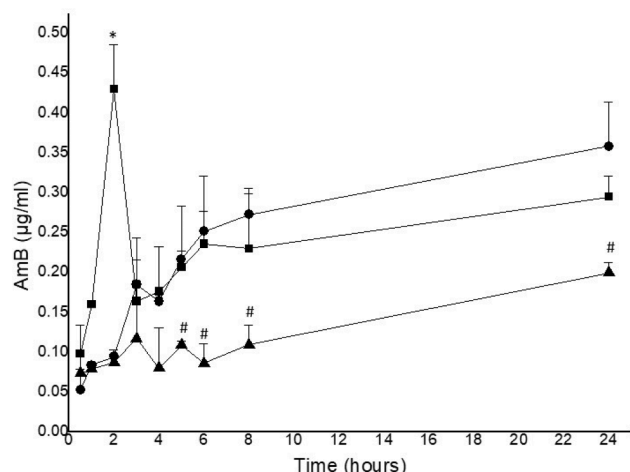


Fig. 5. *In vitro* release profile of F1, F2 and unprocessed AmB. Key: ■- F1; ●- F2 and ▲- raw AmB. Statistical differences are represented by \*  $p < 0.05$  F1 versus F2 and raw AmB; #  $p < 0.05$  F1 and F2 versus raw AmB.

and 5 and 14-fold higher than dimeric AmB at the same time points ( $p < 0.05$ ). F2 uptake was similar to dimeric AmB except at longer time points (24 h) ( $p < 0.05$ ) (Fig. 8). At 1 h, no statistically significant differences were observed amongst the three formulations when tested at intermediate concentrations (0.4–1.56  $\mu\text{g/ml}$ ). However, differences between the formulations were clearly noticeable at low (0.2  $\mu\text{g/ml}$ ) and high concentrations (3.125  $\mu\text{g/ml}$ ). F1 showed a prominent faster uptake at low concentrations compared to F2 and dimeric AmB, which may be related to its larger particle size in dispersion (20-fold greater), making the F1 formulation more attractive for macrophage uptake (Fig. S7, Supplementary material). Dimeric AmB showed a sharp decrease in uptake at high concentrations. This may be the result of a saturation process. However, both F1 and F2 formulations contain mannose which can bind to the receptors located on the surface of the macrophages and overall, enhance macrophage uptake even at higher concentrations.

### 3.9. Pharmacokinetic profile

The pharmacokinetic profile of F1 and F2 after intratracheal administration at 5 mg/kg is illustrated in Fig. 9. Greater concentrations of AmB remained in the ELF after 72 h of F1 administration compared to F2 which can be attributed to the semicrystalline nature of the F1 material and larger particle size in liquid dispersion. In contrast, F2 due to its amorphous nature is more water-soluble being more permeable across the pulmonary epithelial cells and hence, the AmB values in the ELF decrease faster. In both formulations, total plasma concentrations above 1  $\mu\text{g/ml}$  were maintained for at least 24 h, indicating that a single daily pulmonary administration would be enough to elicit a prophylactic or therapeutic effect against *Aspergillus* spp. (Elefanti et al., 2013a, 2013b).

In contrast, AmB total plasma levels dropped after 48 h of the intravenous administration of AmBisome® (<1  $\mu\text{g/ml}$  at 4 h) explaining the lack of efficacy of this medicine when parenterally administered in critical ill patients (Fig. 8). This may explain why initial therapy with voriconazole is preferred over AmBisome®, as the former has led to better responses and improved survival rates, and is associated with fewer severe side effects (Herbrecht et al., 2002). No sign of toxicity was observed after a single inhalation. However, further studies should be performed to confirm chronic toxicity after a multiple dose regimen.

### 3.10. Stability studies

According to the modified Arrhenius equation, unprocessed crystalline AmB had an activation energy of  $34.3 \pm 5.4$  kcal/mol. In contrast, F1 had a higher activation energy ( $44.4 \pm 5.4$  Kcal/mol), indicating that greater energy is required to promote its chemical degradation while F2's activation energy was lower ( $13.6 \pm 1.9$  kcal/mol) and indicated poorer chemical stability over time. Experimental data demonstrated that both F1 and F2 formulations were stable over two years (>90 % drug content) under refrigerated and relatively dry conditions (10 % RH). However, F1 was significantly more stable over time compared to F2 at room temperature (Fig. 10). In all cases, both formulations were sensitive to moisture (data not shown) and hence, a moisture protective packaging would be required to prolong their shelf-life. The different degradation kinetic models that best fit the data for F1 and F2 can explain the differences observed in terms of long-term stability. AmB in F2 is degraded following a first order degradation.

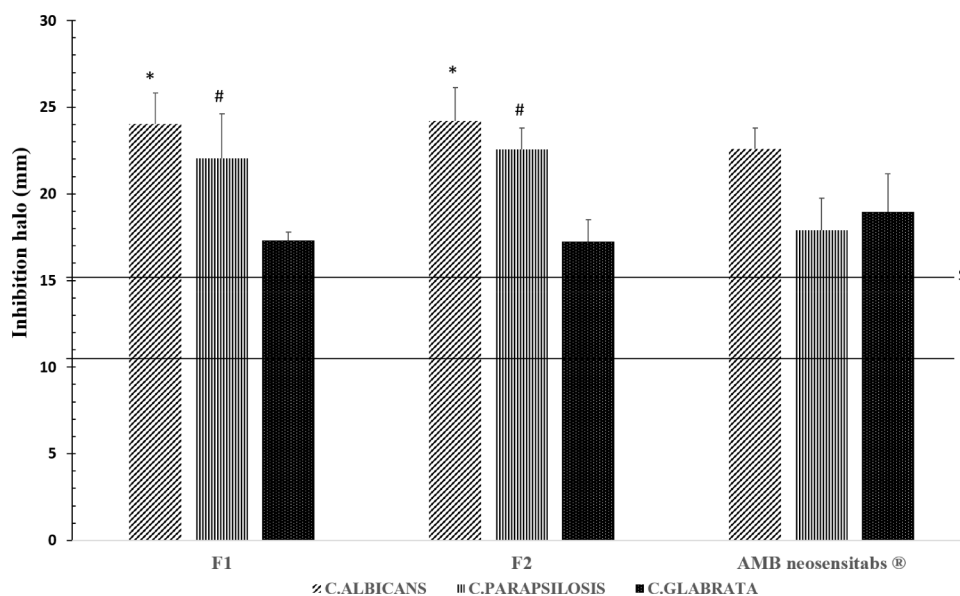
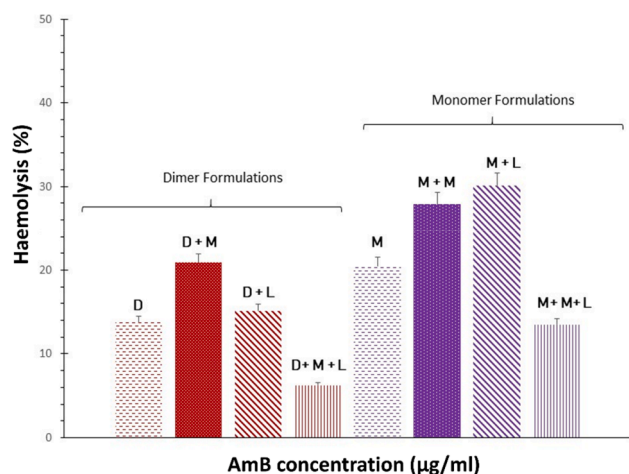


Fig. 6. *In vitro* antifungal activity against *Candida* sp. Key: statistical differences ( $p < 0.05$ ) in *C. albicans* and *C. parapsilosis* are represented by \* and # respectively compared to commercial AmB Neo-Sensitabs® disks.



**Fig. 7.** *In vitro* haemolysis of dimeric AmB formulations (tested at 62.5 µg/ml) and monomeric formulations tested at 25 µg/ml. Key: dimer (D); dimer + mannose (D + M); dimer + leucine (D + L); dimer + leucine + mannose (D + M + L); monomer (M); monomer + mannose (M + M); monomer + leucine (M + L) and monomer + mannose and leucine (M + M + L).

However, the degradation of AmB in F1 is better explained by an Avrami kinetic model which is pseudo-first order kinetics, consisting of a period of no degradation followed by a quick degradation process (Table S4 in Supplementary material). This may be attributed to the more crystalline nature of F1 which allows the drug to be stabilised in the crystalline domains before the degradation process starts.

#### 4. Discussion

The application of QbD and DoE to the development of a pulmonary AmB formulation has resulted in F1 and F2 optimised AmB DPI formulations, manufactured from Generally Regarded as Safe (GRAS) excipients with suitable aerodynamic particle size for lung deposition. Both formulations were prepared by spray drying and contain a 1:1 AmB:CD weight ratio, a similar content of leucine (10–13 %), but a markedly different amount of mannose (5-fold greater for F1 compared to F2).

The excipients were carefully chosen for the preparation of these AmB DPI formulations. CD was selected preferentially over DOC due to its safety profile and also to because of its ability to solubilise and diffuse across mucus, which can act as a barrier hampering drug efficacy in

pulmonary infections (Loftsson, 2012). Also, CD possesses the ability to remove the biofilm formed by bacteria/fungal cells (Alayande et al., 2016). Cyclodextrins, at high doses, can increase drug permeability by a direct action on mucosal membranes, can enhance drug bioavailability due to the formation of hydrophilic complexes with AmB and can cause perturbation of membrane integrity. Unlike detergents, cyclodextrins solubilise membrane components without entering into the membrane, and therefore their perturbing effects are mild and reversible (Challa et al., 2005). In spite of their low absorption via mucosal membranes, cyclodextrins may also facilitate their own absorption at high concentrations. Therefore, it is not advisable to administer doses above 20 mg/kg (EMA; European Medicines Board, 2017).

Based on this fact and the results from previous solubility studies with AmB in which at least a 1:50 AmB:CD ratio was required to keep the drug solubilised in aqueous media (Ruiz et al., 2014), three different levels of AmB:CD were tested. 1:1, 1:50 and 1:100. DoE studies showed a better performance of the formulation when the lowest AmB:CD weight ratio (1:1) was used. In this condition, in the liquid state, the AmB will be partially solubilised within the CD. This promotes a dynamic equilibrium between aggregated and solubilised AmB by forming inclusion complexes and interplanar H-bonding interactions (Fernandez-Garcia et al., 2022). The partial solubilisation of the AmB can result in a fast action derived from the solubilised drug and a controlled release and prolonged retention in the respiratory tract from the unsolubilised fraction. In our opinion, this equilibrium is preferred for longer efficacy over having the drug totally solubilised. In light of this equilibrium, linked to the fact that lower doses of CD are required to avoid toxicity, the 1:1 AmB:CD weight ratio was considered the most suitable for the development of a pulmonary AmB formulation.

In order to improve the flowability and aerosolisation performance, L-leucine was incorporated in the formulation. Previous studies have demonstrated the anti-adherent properties conferred by leucine which can be associated to the formation of particles with appropriate corrugation during spray drying (Focaroli et al., 2019; Molina et al., 2018). Corrugated particles were observed in the SEM micrographs for both F1 and F2. However, it was critical to know the percentage required within the formulation to obtain easy-flowing particles but at the same time, not to dilute the overall AmB load, taking into account that doses required to treat pulmonary aspergillosis can be high. The percentage of leucine required to keep optimal aerodynamic flow properties in F1 and F2 DPI powder formulations ranged from 10 to 13 %, which is low considering the amounts previously reported by other authors (up to 60 % of the total formulation weight) (Mangal et al., 2018; Yang et al.,

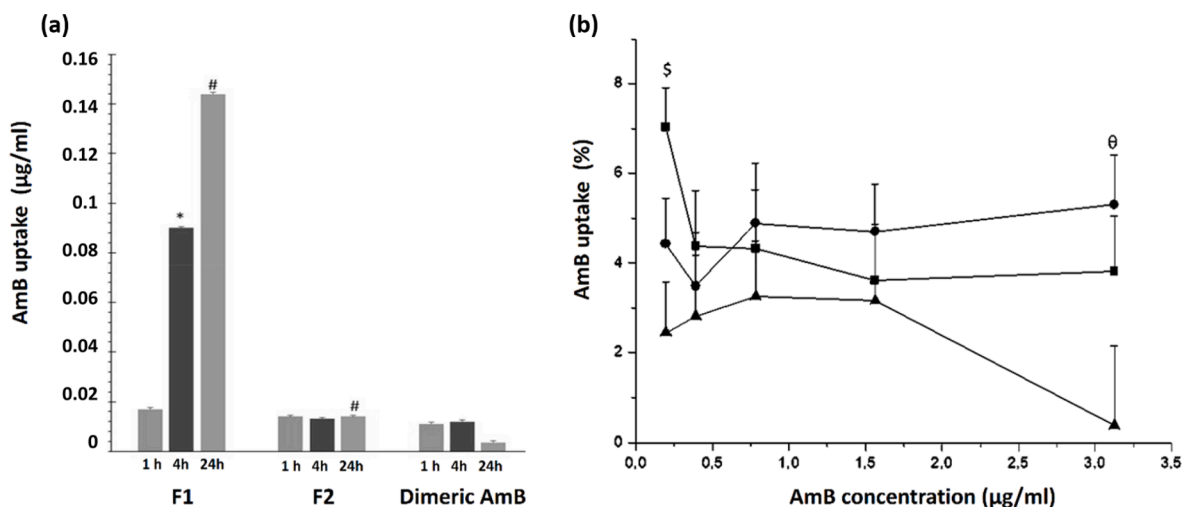


**Fig. 8.** *In vitro* macrophage uptake. (a) Uptake in macrophages using an AmB concentration of 1.56 µg/ml AmB at 1, 4 and 24 h. Key: Statistical differences \*  $p < 0.05$  versus F2 and dimeric AmB, #  $p < 0.05$  versus dimeric AmB. (b) Uptake at different AmB concentrations after 1 h of incubation. Key: -■- F1; -●- F2 and -▲- Dimeric AmB. \$  $p < 0.05$  F1 versus F2 and dimeric AmB; θ  $p < 0.05$  F2 versus dimeric AmB.

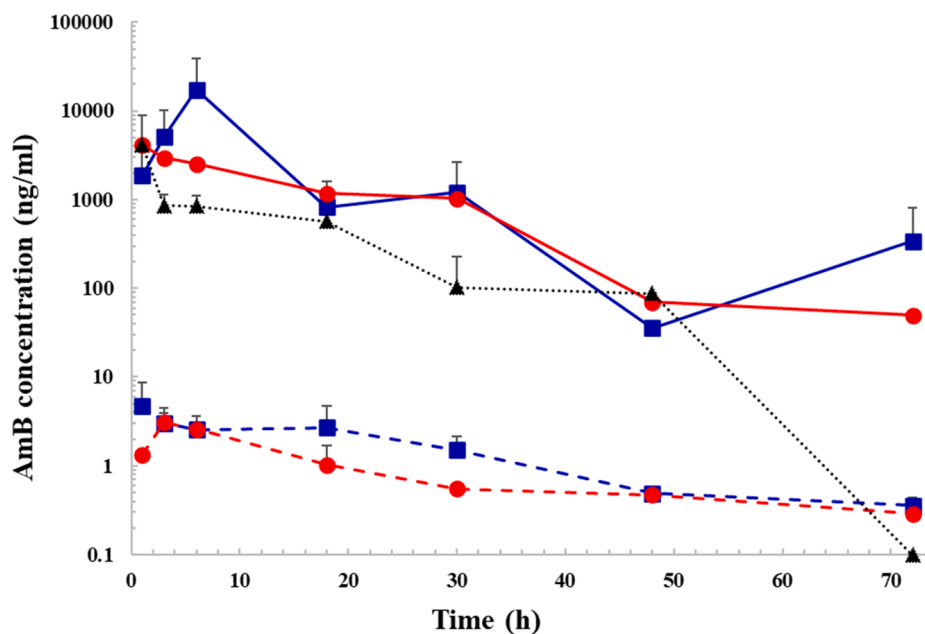


Fig. 9. Pharmacokinetic profile after intratracheal administration of F1 (blue line) and F2 (red line) at 5 mg/kg in OFA-rats compared with the iv administration of Ambisome® (-▲-)(5 mg/kg). Key: — AmB concentration in plasma and - - AmB concentration in ELF. (For interpretation of the references to colour in this figure legend, the reader is referred to the web version of this article.)

2014). Apart from improving the flow properties, leucine was introduced into the DPI formulations to overcome hygroscopicity issues and to protect the formulations against moisture-induced changes (Mah et al., 2019). In fact, F2, which contains 2 % more leucine than F1 showed a less pronounced water uptake in the DVS isotherm profile. Leucine is a hydrophobic amino acid, considered to be safe for use as an excipient in pulmonary formulations. The reason behind its ability to reduce moisture uptake is due to its enrichment at the particle surface of particles during the spray drying process, providing a shell or barrier to moisture ingress (Cui et al., 2018; Otake et al., 2016).

The third key excipient incorporated in the DPI formulations was mannose, a hexose carbohydrate, due to its chemotactic behaviour. It is well-known that glycoproteins influence T cell immune responses to a wide variety of antigens. The polysaccharide-rich cell wall in fungi is the main source of pathogen-associated molecular patterns which are recognised by carbohydrate-binding receptors (CBR), highly expressed on front-line immune cells, mainly macrophages (macrophage mannose receptor) and dendritic cells (Brown, 2006). Recognition of fungal-surface polysaccharides initiates immediate responses such as phagocytosis, production of antimicrobial compounds and induction of pro-inflammatory cytokines that recruit other immune cells (Pinto, Barreto-Bergter, & Taborda, 2008). CBR affinity for sugars is diverse, but mannose is the most common monosaccharide recognized by this receptor (Stahl & Ezekowitz, 1998), and for this reason was chosen as an excipient bearing in mind that, to clear a fungal respiratory infection, a combined action between the drug and the immune system is necessary.

An additional advantage of incorporating mannose into the formulation relates to its potential use for the treatment of visceral leishmaniasis. *Leishmania* is an intracellular parasite which accumulates inside macrophages, leading to a mortal disease if left untreated. This disease affects people from low-income countries in particular, and its effective treatment currently relies on parenterally administered medicines as well as miltefosine, a teratogenic oral formulation (Smith et al., 2018). The lack of non-parenteral effective and safer treatments indicates a major clinical need exists. Several novel oral formulations are under development (Serrano et al., 2015); however, there are still in preclinical or clinical status. The current work, represents the first time the pulmonary co-administration of AmB, a highly potent drug against

*Leishmania* (Corral et al., 2014) and mannose (a chemotactic molecule for macrophages) has been proposed for the treatment of leishmaniasis. Further studies need to be performed to investigate accumulation in the main target organs, liver and spleen. However, the pulmonary administration of AmB could be of great therapeutic advantage to patients with post Kala azar leishmaniasis in which case parasites are disseminated in the body reaching pulmonary septa, alveoli and bronchoalveolar fluid (Cheepsattayakorn & Cheepsattayakorn, 2014; Russo et al., 2003).

From a pharmacotechnical point of view, mannose acted as a switch from amorphous to semi-crystalline AmB powder formulations. In fact, the main difference between the composition of F1 and F2 is the percentage of mannose. The use of a low percentage of mannose in F2 (AmB:mannose, 1:0.2, W:W) resulted in an AmB composite material that was amorphous in nature, while greater ratios of mannose employed in F1 (1:1, AmB:mannose) triggered partial AmB crystallisation leading to a semi-crystalline formulation. The difference in amorphous or semi-crystalline solid state between F1 and F2 was demonstrated to have a large impact on the physicochemical properties of the DPI powder. It is worth highlighting that F1 is a less cohesive powder with easier wettability, higher supersaturation at earlier time points in aqueous medium, greater chemical stability (>2 years at room temperature) and a more robust lung deposition at different air flow rates, compared to F2. In contrast, F2, due to its amorphous nature, is more sensitive under storage to chemical degradation and aggregation. This can explain the differences observed in the lung deposition at the different air flow rates and the higher retention in the Handihaler device and upper regions of the impactor apparatus such as the mouthpiece adaptor and the induction port.

Overall, a robust lung deposition pattern with small differences at different air flow rates is key for the success of an AmB pulmonary DPI formulation, taking into account that most patients would suffer from respiratory infections and in many cases their breathing capacity may be compromised. For this reason, a fixed-dose combination DPI powder containing AmB and SS was also developed, designed, in particular, for those patients in critical care that may require both an antifungal and a bronchodilator drug.

The particle size of F1 when dispersed in aqueous medium is much larger than F2 which explains the greater retention in the ELF after

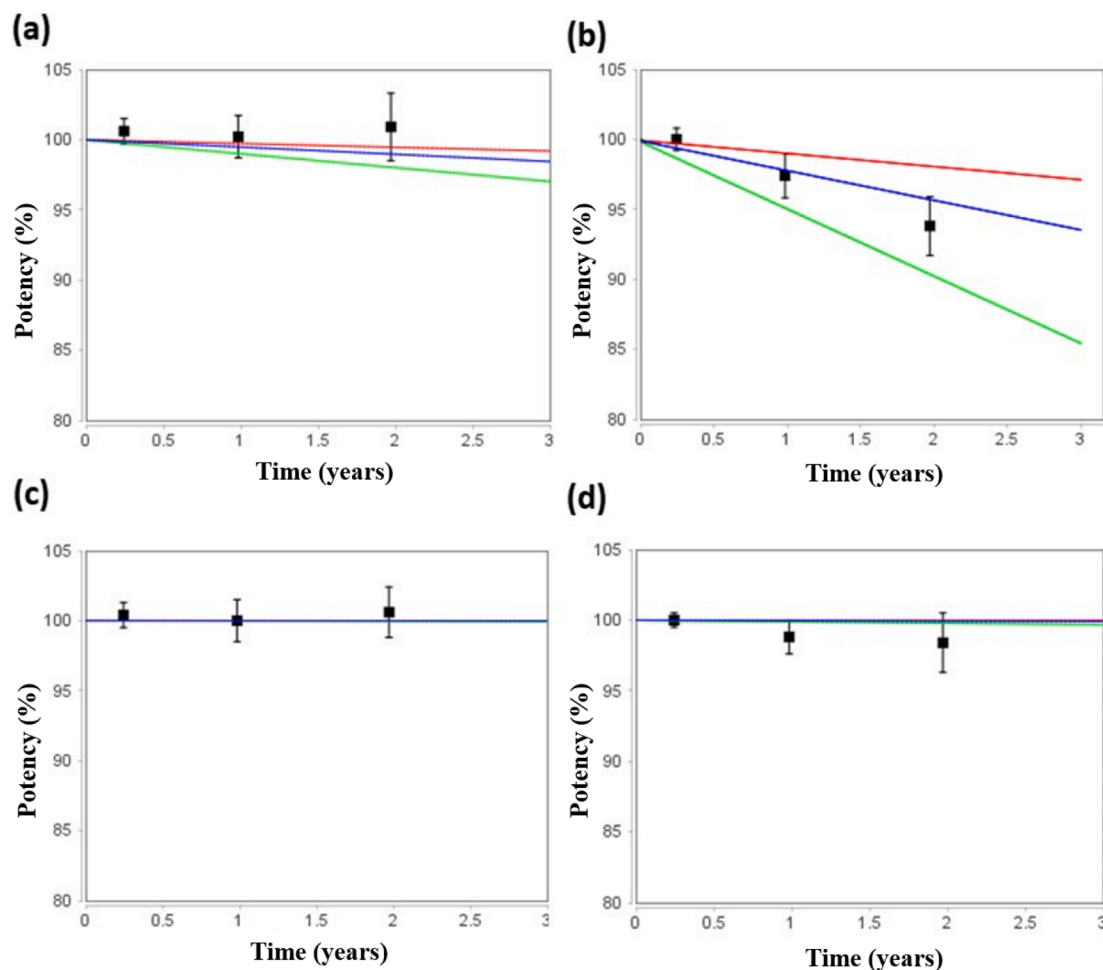


**Fig. 10.** Predicted vs experimental long term stability results (over 3, 12 and 24 months) of F1 and F2 DPIs. Key: (a) F1 at 25 °C/10 % RH, (b) F2 at 25 °C/10 % RH (c) F1 at 4 °C/10 % RH and (d) F2 at 4 °C/10 % RH. Key: ■ - Experimental data points. Blue line represents the predicted mean stability at a certain condition and the red and green lines display 95 % confident intervals. (For interpretation of the references to colour in this figure legend, the reader is referred to the web version of this article.)

intratracheal administration and the enhanced macrophage uptake. However, F2 has a smaller particle size upon reconstitution which facilitates permeability across the epithelial lung cells, providing a faster decrease in AmB levels in the ELF after pulmonary administration. Nevertheless, the AmB levels in the respiratory tract for both formulations were much greater than those achieved by parenterally administered AmBisome®. This shows the need to tailor drug formulations for the required administration route, especially in the case of AmB where the off targeted side effects on tissues such as kidneys can lead to the suppression of the therapy. The dual combination of mannose and leucine resulted in a reduction in the second more severe adverse effect caused by AmB, haemolysis. The reduced haemolytic toxicity of F1 and F2 along with prolonged retention time (>24 h) in the respiratory tract with concentrations above the IC<sub>50</sub> against *Aspergillus* (Elefanti et al., 2013a) are a great therapeutic advantage compared to other current treatments employed in clinical practice for pulmonary fungal infections.

To date, most clinical trials concerning AmB pulmonary administration have been focused on the safety and efficacy of inhaled lipidic marketed AmB formulations (AmBisome® and Abelcet®). These formulations are intended for parenteral use and they are employed off-label after reconstitution, by nebulisation for the prevention or treatment of pulmonary aspergillosis colonisation (ClinicalTrials.gov., 2019). However, experience with inhaled antibiotics designed for parenteral administration showed that these formulations can cause significant bronchial irritation due to the use of non-pulmonary

physiological excipients in their composition such as high content of dextrose required for lyophilisation (Quon, Goss, & Ramsey, 2014). Previous studies have pointed to the fact that manufacturing of AmB liposomes by reverse-phase evaporation using organic solvents may be responsible for the potential toxicity of the inhaled powder, due to residual solvents in the formulation, and that furthermore, the low AmB loading capacity of such liposome formulations may make them ineffective in the treatment of fungal lung infections (Shah & Misra, 2004).

Not only is there a clinical need for antifungal DPI formulations, but there also exists a need for combined DPI formulations for the treatment of fungal pulmonary infections and bronchoconstriction. This need is demonstrated by the clinical trials that are currently ongoing. For maintenance of remission in allergic broncho pulmonary aspergillosis, a randomized controlled trial of inhaled nebulized AmB (10 mg) and nebulized budesonide (1 mg) administered twice a day, three times a week over 4 months has been approved (ClinicalTrials.gov., 2015). Even though, clinical results have not been published yet, this proves the clinical need for an inhaled combined therapy, as there is currently no marketed fixed dose combination DPI product for this purpose.

## 5. Conclusions

The combination of AmB-CD-leucine and mannose in appropriate amounts has led to the development of effective and safer DPI formulations for the treatment of pulmonary fungal infections. The F1

optimised semicrystalline formulation, consisting of 29.8 % AmB, 29.8 %  $\gamma$ -CD, 29.8 % mannose and 10.4 % leucine, showed a greater FPF below 5 and 3  $\mu\text{m}$  at different air flow rates, longer stability at refrigerated and room temperature conditions and higher retention times after intratracheal *in vivo* administration compared to the F2 amorphous formulation. Also, the F1 formulation exhibited a larger macrophage uptake, which could be of great benefit in the treatment of disseminated visceral leishmaniasis affecting the lung. Both optimised formulations are versatile and easily adapted to patients' needs as they have shown good *in vitro* deposition patterns from both a DPI and, after reconstitution, a nebuliser. The development of the fixed dose AmB-SS combination DPI formulation is an interesting approach for the treatment of fungal pulmonary infections that cause or co-exist with bronchoconstriction.

#### CRedit authorship contribution statement

**E. de Pablo:** Investigation, Writing – original draft. **P. O’Connell:** Investigation. **R. Fernández-García:** Investigation. **S. Marchand:** Investigation, Resources. **A. Chauzy:** Investigation. **Frederic Tewes:** Resources. **M.A. Dea-Ayuela:** Investigation. **Dinesh Kumar:** Investigation. **F. Bolás:** . **M.P. Ballesteros:** Writing – review & editing, Supervision. **J.J. Torrado:** Writing – review & editing, Supervision. **A.M. Healy:** Resources, Writing – review & editing, Funding acquisition. **D.R. Serrano:** Conceptualization, Investigation, Resources, Writing – original draft, Writing – review & editing, Supervision, Funding acquisition.

#### Declaration of Competing Interest

The authors declare that they have no known competing financial interests or personal relationships that could have appeared to influence the work reported in this paper.

#### Data availability

Data will be made available on request.

#### Acknowledgement

This study was partially supported by the Complutense University of Madrid and Science Foundation Ireland grants co-funded under the European Regional Development Fund (SFI/12/RC/2275 and SFI/12/RC/) awarded to Prof. A. M. Healy. This work has benefited from the facilities and expertise of PREBIOS platform (University of Poitiers). This study has been also funded by the Spanish Ministry of Science and Innovation (award PID2021-126310OA-I00 to Dolores Serrano).

#### Appendix A. Supplementary material

Supplementary data to this article can be found online at <https://doi.org/10.1016/j.ijpharm.2023.122788>. DoE matrix, shelf-life prediction, antiparasitic activity, Fish bone diagram and additional DSC thermograms and MMAD characterization data is found in Supplementary material.

#### References

- Ader, F., Nseir, S., Le Berre, R., Leroy, S., Tillie-Leblond, I., Marquette, C.H., Durocher, A., 2005. Invasive pulmonary aspergillosis in chronic obstructive pulmonary disease: an emerging fungal pathogen. *Clin. Microbiol. Infect.* 11 (6), 427–429.
- Alayande, A.B., Kim, L.H., Kim, I.S., 2016. Cleaning efficacy of hydroxypropyl-beta-cyclodextrin for biofouling reduction on reverse osmosis membranes. *Biofouling* 32 (4), 359–370.
- Berkenfeld, K., Lamprecht, A., McConville, J.T., 2015. Devices for dry powder drug delivery to the lung. *AAPS PharmSciTech* 16 (3), 479–490.
- Bilbao-Ramos, P., Sifontes-Rodriguez, S., Dea-Ayuela, M.A., Bolas-Fernandez, F., 2012. A fluorometric method for evaluation of pharmacological activity against intracellular Leishmania amastigotes. *J. Microbiol. Methods* 89 (1), 8–11.
- Broeders, M.E., Molema, J., Hop, W.C., Folgering, H.T., 2005. Salbutamol pMDI gives less protection to methacholine induced airway obstruction than salbutamol via spacer or DPI. *Eur. J. Clin. Pharmacol.* 60 (12), 837–841.
- Brown, G.D., 2006. Dectin-1: a signalling non-TLR pattern-recognition receptor. *Nat. Rev. Immunol.* 6 (1), 33–43.
- Challa, R., Ahuja, A., Ali, J., Khar, R.K., 2005. Cyclodextrins in drug delivery: an updated review. *AAPS PharmSciTech* 6 (2), E329–E357.
- Cheepsattayakorn, A., Cheepsattayakorn, R., 2014. Parasitic pneumonia and lung involvement. *Biomed Res. Int.* 2014, 874021.
- Chenoweth, C.E., Singal, S., Pearson, R.D., Betts, R.F., Markovitz, D.M., 1993. Acquired immunodeficiency syndrome-related visceral leishmaniasis presenting in a pleural effusion. *Chest* 103 (2), 648–649.
- Chono, S., Tanino, T., Seki, T., Morimoto, K., 2006. Influence of particle size on drug delivery to rat alveolar macrophages following pulmonary administration of ciprofloxacin incorporated into liposomes. *J. Drug Target.* 14 (8), 557–566.
- ClinicalTrials.gov., 2015. <https://clinicaltrials.gov/ct2/show/NCT01857479>.
- ClinicalTrials.gov., 2019. <https://clinicaltrials.gov/ct2/results?cond=amphotericin+B+inhalation&term=&cntry=&state=&city=&dist=>.
- Corral, M.J., Serrano, D.R., Moreno, I., Torrado, J.J., Dominguez, M., Alunda, J.M., 2014. Efficacy of low doses of amphotericin B plus allicin against experimental visceral leishmaniasis. *J. Antimicrob. Chemother.* 69 (12), 3268–3274.
- Corrigan, D.O., Healy, A.M., Corrigan, O.I., 2006. Preparation and release of salbutamol from chitosan and chitosan co-spray dried compacts and multiparticulates. *Eur. J. Pharm. Biopharm.* 62 (3), 295–305.
- Cui, Y., Zhang, X., Wang, W., Huang, Z., Zhao, Z., Wang, G., Wu, C., 2018. Moisture-resistant co-spray-dried netilmicin with l-leucine as dry powder inhalation for the treatment of respiratory infections. *Pharmaceutics* 10 (4).
- Curtin, V., Amharar, Y., Gallagher, K.H., Corcoran, S., Tajber, L., Corrigan, O.I., Healy, A.M., 2013. Reducing mechanical activation-induced amorphisation of salbutamol sulphate by co-processing with selected carboxylic acids. *Int. J. Pharm.* 456 (2), 508–516.
- Antony J. Cutler, K. A. D. (1998). *Encyclopedia of Immunology (Second Edition)*.
- de Pablo, E., Fernandez-Garcia, R., Ballesteros, M.P., Torrado, J.J., Serrano, D.R., 2017. Nebulised antibiotherapy: conventional versus nanotechnology-based approaches, is targeting at a nano scale a difficult subject? *Ann. Transl. Med.* 5 (22), 448.
- Dea-Ayuela, M.A., Castillo, E., Gonzalez-Alvarez, M., Vega, C., Rolon, M., Bolas-Fernandez, F., Gonzalez-Rosende, M.E., 2009. In vivo and in vitro anti-leishmanial activities of 4-nitro-N-pyrimidin- and N-pyrazin-2-ylbenzenesulfonamides, and N2-(4-nitrophenyl)-N1-propylglycinamide. *Bioorg. Med. Chem.* 17 (21), 7449–7456.
- Dickinson, P.A., Howells, S.W., Kellaway, I.W., 2001. Novel nanoparticles for pulmonary drug administration. *J. Drug Target.* 9 (4), 295–302.
- DrugPatentWatch, (27/09/2010). Drug Patent Expirations and Intelligent Drug Patent Watch. <http://www.drugpatentwatch.com>.
- European Medicines Board guideline on cyclodextrin use in humans. Available at: [https://www.ema.europa.eu/en/documents/scientific-guideline/questions-answers-cyclodextrins-used-excipients-medicinal-products-human-use\\_en.pdf](https://www.ema.europa.eu/en/documents/scientific-guideline/questions-answers-cyclodextrins-used-excipients-medicinal-products-human-use_en.pdf) (2017).
- Elefanti, A., Mouton, J.W., Krompa, K., Al-Saigh, R., Verweij, P.E., Zerva, L., Meletiadis, J., 2013a. Inhibitory and fungicidal effects of antifungal drugs against *Aspergillus* species in the presence of serum. *Antimicrob. Agents Chemother.* 57 (4), 1625–1631.
- Elefanti, A., Mouton, J.W., Verweij, P.E., Tsakris, A., Zerva, L., Meletiadis, J., 2013b. Amphotericin B- and voriconazole-echinocandin combinations against *Aspergillus* spp.: effect of serum on inhibitory and fungicidal interactions. *Antimicrob. Agents Chemother.* 57 (10), 4656–4663.
- EMA., I. M. A. a. [https://www.ema.europa.eu/en/medicines?search\\_api\\_views\\_fulltext=INHALED+MEDICINES](https://www.ema.europa.eu/en/medicines?search_api_views_fulltext=INHALED+MEDICINES). Accessed date: 29/04/2018.
- Espada, R., Valdespina, S., Alfonso, C., Rivas, G., Ballesteros, M.P., Torrado, J.J., 2008. Effect of aggregation state on the toxicity of different amphotericin B preparations. *Int. J. Pharm.* 361 (1–2), 64–69.
- Fernandez-Garcia, R., de Pablo, E., Ballesteros, M.P., Serrano, D.R., 2017. Unmet clinical needs in the treatment of systemic fungal infections: the role of amphotericin B and drug targeting. *Int. J. Pharm.* 525 (1), 139–148.
- Fernandez-Garcia, R., Munoz-Garcia, J.C., Wallace, M., Fabian, L., Gonzalez-Burgos, E., Gomez-Serranillos, M.P., Serrano, D.R., 2022. Self-assembling, supramolecular chemistry and pharmacology of amphotericin B: Poly-aggregates, oligomers and monomers. *J. Control. Release* 341, 716–732.
- Focaroli, S., Mah, P.T., Hastedt, J.E., Gitlin, I., Oscarson, S., Fahy, J.V., Healy, A.M., 2019. A Design of Experiment (DoE) approach to optimise spray drying process conditions for the production of trehalose/leucine formulations with application in pulmonary delivery. *Int. J. Pharm.* 562, 228–240.
- Grossjohann, C., Serrano, D.R., Paluch, K.J., O’Connell, P., Vella-Zarb, L., Manesiotis, P., Healy, A.M., 2015. Polymorphism in sulfadimidine/4-aminosalicylic acid cocrystals: solid-state characterization and physicochemical properties. *J. Pharm. Sci.* 104 (4), 1385–1398.
- Guebitz, B., Schnedl, H., Khinast, J.G., 2012. A risk management ontology for Quality-by-Design based on a new development approach according GAMP 5.0. *Expert Syst. Appl.* 39, 7291–7301.
- Herbrecht, R., Denning, D.W., Patterson, T.F., Bennett, J.E., Greene, R.E., Oestmann, J. W., Invasive Fungal Infections Group of the European Organisation for Research and Treatment of Cancer and the Global Aspergillus Study Group, 2002. Voriconazole versus amphotericin B for primary therapy of invasive aspergillosis. *N. Engl. J. Med.* 347 (6), 408–415.



- Lamy, B., Tewes, F., Serrano, D.R., Lamarche, I., Gobin, P., Couet, W., Marchand, S., 2018. New aerosol formulation to control ciprofloxacin pulmonary concentration. *J. Control. Release* 271, 118–126.
- Lamy, B., Serrano, D.R., O'Connell, P., Couet, W., Marchand, S., Healy, A.M., Tewes, F., 2019. Use of leucine to improve aerodynamic properties of ciprofloxacin-loaded maltose microparticles for inhalation. *Eur. J. Pharm. Res.* 1 (1), 2–11.
- Loftsson, T., 2012. Drug permeation through biomembranes: cyclodextrins and the unstirred water layer. *Pharmazie* 67 (5), 363–370.
- Mah, P.T., O'Connell, P., Focaroli, S., Lundy, R., O'Mahony, T.F., Hastedt, J.E., Healy, A.M., 2019. The use of hydrophobic amino acids in protecting spray dried trehalose formulations against moisture-induced changes. *Eur. J. Pharm. Biopharm.* 144, 139–153.
- Mangal, S., Nie, H., Xu, R., Guo, R., Cavallaro, A., Zemlyanov, D., Zhou, Q.T., 2018. Physico-chemical properties, aerosolization and dissolution of co-spray dried azithromycin particles with L-leucine for inhalation. *Pharm. Res.* 35 (2), 28.
- Molina, C., Kajaly, W., Chen, Q., Commandeur, D., Nokhodchi, A., 2018. Agglomerated novel spray-dried lactose-leucine tailored as a carrier to enhance the aerosolization performance of salbutamol sulfate from DPI formulations. *Drug Deliv. Transl. Res.* 8 (6), 1769–1780.
- Ordóñez-Gutiérrez, L., Espada-Fernández, R., Dea-Ayuela, M.A., Torrado, J.J., Bolas-Fernández, F., Alunda, J.M., 2007. In vitro effect of new formulations of amphotericin B on amastigote and promastigote forms of *Leishmania infantum*. *Int. J. Antimicrob. Agents* 30 (4), 325–329.
- Otake, H., Okuda, T., Hira, D., Kojima, H., Shimada, Y., Okamoto, H., 2016. Inhalable spray-freeze-dried powder with L-leucine that delivers particles independent of inspiratory flow pattern and inhalation device. *Pharm. Res.* 33 (4), 922–931.
- Orphan designation: Amphotericin B (for inhalation use) for: Prevention of pulmonary fungal infection in patients deemed at risk. (28/08/2006 updated).** <https://www.ema.europa.eu/en/medicines/human/orphan-designations/eu306391>.
- Paranjpe, M., Müller-Goymann, C.C., 2014. Nanoparticle-mediated pulmonary drug delivery: a review. *Int. J. Mol. Sci.* 15 (4), 5852–5873.
- Park, C.W., Li, X., Vogt, F.G., Hayes Jr., D., Zwischenberger, J.B., Park, E.S., Mansour, H.M., 2013. Advanced spray-dried design, physicochemical characterization, and aerosol dispersion performance of vancomycin and clarithromycin multifunctional controlled release particles for targeted respiratory delivery as dry powder inhalation aerosols. *Int. J. Pharm.* 455 (1–2), 374–392.
- Pinto, M.R., Barreto-Bergter, E., Taborda, C.P., 2008. Glycoconjugates and polysaccharides of fungal cell wall and activation of immune system. *Braz. J. Microbiol.* 39 (2), 195–208.
- Quon, B.S., Goss, C.H., Ramsey, B.W., 2014. Inhaled antibiotics for lower airway infections. *Ann. Am. Thorac. Soc.* 11 (3), 425–434.
- Rijnders, B.J., Cornelissen, J.J., Slobbe, L., Becker, M.J., Doorduijn, J.K., Hop, W.C., de Marie, S., 2008. Aerosolized liposomal amphotericin B for the prevention of invasive pulmonary aspergillosis during prolonged neutropenia: a randomized, placebo-controlled trial. *Clin. Infect. Dis.* 46 (9), 1401–1408.
- Rojek, B., Wesolowski, M., 2019. FTIR and TG analyses coupled with factor analysis in a compatibility study of acetazolamide with excipients. *Spectrochim. Acta A: Mol. Biomol. Spectrosc.* 208, 285–293.
- Rolon, M., Serrano, D.R., Lalatsa, A., de Pablo, E., Torrado, J.J., Ballesteros, M.P., Dea-Ayuela, M.A., 2017. Engineering Oral and parenteral amorphous amphotericin B formulations against experimental *Trypanosoma cruzi* infections. *Mol. Pharm.* 14 (4), 1095–1106.
- Ruiz, H.K., Serrano, D.R., Dea-Ayuela, M.A., Bilbao-Ramos, P.E., Bolas-Fernández, F., Torrado, J.J., Molero, G., 2014. New amphotericin B-gamma cyclodextrin formulation for topical use with synergistic activity against diverse fungal species and *Leishmania* spp. *Int. J. Pharm.* 473 (1–2), 148–157.
- Russo, R., Laguna, F., Lopez-Velez, R., Medrano, F.J., Rosenthal, E., Cacopardo, B., Nigro, L., 2003. Visceral leishmaniasis in those infected with HIV: clinical aspects and other opportunistic infections. *Ann. Trop. Med. Parasitol.* 97 (Suppl. 1), 99–105.
- Salzano, G., Wankar, J., Ottani, S., Villemagne, B., Baulard, A.R., Willand, N., Gref, R., 2017. Cyclodextrin-based nanocarriers containing a synergic drug combination: a potential formulation for pulmonary administration of antitubercular drugs. *Int. J. Pharm.* 531 (2), 577–587.
- Serrano, D.R., Hernandez, L., Fleire, L., Gonzalez-Alvarez, I., Montoya, A., Ballesteros, M.P., Torrado, J.J., 2013. Hemolytic and pharmacokinetic studies of liposomal and particulate amphotericin B formulations. *Int. J. Pharm.* 447 (1–2), 38–46.
- Serrano, D.R., Lalatsa, A., Dea-Ayuela, M.A., Bilbao-Ramos, P.E., Garrett, N.L., Moger, J., Uchegbu, I.F., 2015. Oral particle uptake and organ targeting drives the activity of amphotericin B nanoparticles. *Mol. Pharm.* 12 (2), 420–431.
- Serrano, D.R., O'Connell, P., Paluch, K.J., Walsh, D., Healy, A.M., 2016a. Cocrystal habit engineering to improve drug dissolution and alter derived powder properties. *J. Pharm. Pharmacol.* 68 (5), 665–677.
- Serrano, D.R., Persoons, T., D'Arcy, D.M., Galiana, C., Dea-Ayuela, M.A., Healy, A.M., 2016b. Modelling and shadowgraph imaging of cocrystal dissolution and assessment of in vitro antimicrobial activity for sulfadiazine/4-aminosalicylic acid cocrystals. *Eur. J. Pharm. Sci.* 89, 125–136.
- Serrano, D.R., Walsh, D., O'Connell, P., Mugheirbi, N.A., Worku, Z.A., Bolas-Fernandez, F., Healy, A.M., 2018. Optimising the in vitro and in vivo performance of oral cocrystal formulations via spray coating. *Eur. J. Pharm. Biopharm.* 124, 13–27.
- Serrano, D.R., Fernandez-Garcia, R., Mele, M., Healy, A.M., Lalatsa, A., 2019. Designing fast-dissolving orodispersible films of amphotericin B for oropharyngeal candidiasis. *Pharmaceutics* 11 (8).
- Shah, S.P., Misra, A., 2004. Development of liposomal amphotericin B dry powder inhaler formulation. *Drug Deliv.* 11 (4), 247–253.
- Shukla, A., Mishra, V., Bhoop, B.S., Katore, O.P., 2015. Alginate coated chitosan microparticles mediated oral delivery of diphtheria toxoid. Part A. Systematic optimization, development and characterization. *Int. J. Pharm.* 495 (1), 220–233.
- Smith, L., Serrano, D.R., Mauer, M., Bolas-Fernandez, F., Dea-Ayuela, M.A., Lalatsa, A., 2018. Orally bioavailable and effective buparvaquone lipid-based nanomedicines for visceral leishmaniasis. *Mol. Pharm.* 15 (7), 2570–2583.
- Sosnowski, T.R., 2016. Selected engineering and physicochemical aspects of systemic drug delivery by inhalation. *Curr. Pharm. Des.* 22 (17), 2453–2462.
- Stahl, P.D., Ezekowitz, R.A., 1998. The mannose receptor is a pattern recognition receptor involved in host defense. *Curr. Opin. Immunol.* 10 (1), 50–55.
- Suzuki, Y., Shirai, M., Asada, K., Yasui, H., Karayama, M., Hozumi, H., Suda, T., 2018. Macrophage mannose receptor, CD206, predict prognosis in patients with pulmonary tuberculosis. *Sci. Rep.* 8 (1), 13129.
- Tewes, F., Brillault, J., Lamy, B., O'Connell, P., Olivier, J.C., Couet, W., Healy, A.M., 2016. Ciprofloxacin-loaded inorganic-organic composite microparticles to treat bacterial lung infection. *Mol. Pharm.* 13 (1), 100–112.
- Vartiainen, V., Raula, J., Bimbo, L.M., Viinamäki, J., Backman, J.T., Ugur, N., Myllärniemi, M., 2018. Pulmonary administration of a dry powder formulation of the antifibrotic drug tilorone reduces silica-induced lung fibrosis in mice. *Int. J. Pharm.* 544 (1), 121–128.
- Walsh, D., Serrano, D.R., Worku, Z.A., Madi, A.M., O'Connell, P., Twamley, B., Healy, A.M., 2018. Engineering of pharmaceutical cocrystals in an excipient matrix: spray drying versus hot melt extrusion. *Int. J. Pharm.* 551 (1–2), 241–256.
- Waterman, K.C., Swanson, J.T., Lippold, B.L., 2014. A scientific and statistical analysis of accelerated aging for pharmaceuticals. Part 1: accuracy of fitting methods. *J. Pharm. Sci.* 103 (10), 3000–3006.
- Yang, Y., Yang, Z., Ren, Y., Mei, X., 2014. Effects of formulation and operating variables on zanamivir dry powder inhalation characteristics and aerosolization performance. *Drug Deliv.* 21 (6), 480–486.